Determination of the Diffusion Coefficient for CO_2 in Porous Media

A Thesis submitted to the department of mineral resources and petroleum engineering in partial fulfilment of the requirements for the degree of master of science

Tannaz Ahmadi

2012

Department MINERAL RESOURCES & PETROLEUM ENGINEERING
Chair of Reservoir Engineering
Prof. Dr. Stephan K. Matthäi

An
Tannaz Ahmadi
Keplerstraße 75/4
8020 Graz

Max-Tendler Str. 4
8700 Leoben
Austria

Tel.: +43 (0)3842 402-3000
Fax: +43 (0)3842 402-8202

e-mail: stephan.matthäi@unileoben.ac.at

Betreff: **Thesis**

Leoben, am 8. Juni 2011

Sehr geehrte Frau Ahmadi,

Das von der OMV zur Verfügung gestellte Thema der Thesis mit dem Titel
Determination of the Diffusion Coefficient for CO_2 in Porous Media

Wurde Ihnen zur Ausarbeitung übertragen. Die Arbeiten werden von Ihnen in der OMV unter Betreuung von Dr. Klaus Potsch und am Department für Mineral Resources und Petroleum Engineering unter der Betreuung von Herrn Prof. Stephan Matthäi durchgeführt.

Dieses Schreiben wird nach Abschluss der Arbeit mit eingebunden.

Mit freundlichen Grüßen und Glück auf!

Prof. Dr. Stephan K. Matthäi
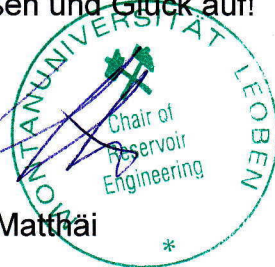
Affidavit

I declare in lieu of oath, that I wrote this thesis and performed the associated research myself, using only literature cited in this volume.

Eidesstattliche Erklärung

Ich erkläre an Eides statt, dass ich diese Arbeit selbstständig verfasst, andere als die angegebenen Quellen und Hilfsmittel nicht benutzt und mich auch sonst keiner unerlaubten Hilfsmittel bedient habe.

October 2012   Tannaz Ahmadi

Abstract

Immobility of heavy oil due to its high viscosity leads to a low recovery in such reservoirs. Carbon dioxide injection can be used to enhance oil recovery by reducing its viscosity as the gas mixes and diffuses into the heavy oil. Better understanding of diffusion coefficient of CO_2, D_{CO_2}, in porous media, which is a significant issue in recovery factor of oil fields is the main objective of my work.

In this thesis, I have analysed the D_{CO_2} in porous media under initial conditions via physical experiments. CO_2 gas was injected into a container/core holder containing water/oil saturated Berea sandstones at temperature of 40, 80°C and pressure of 100 bar.

As the CO_2 molecules start to diffuse in the porous media, the pressure in the system changes. The change of pressure over the time depends on the rate of diffusion that means on the diffusion coefficient and therefore the subsequent pressure decline was monitored to be used in a mathematical form to interpret the diffusion coefficient.

The mathematical model was developed using fick's law combined with gas law and at the end the diffusion coefficient was calculated using pressure profiles coupled with the defined mathematical model.

Preliminary experiments with water/brine were run at pressure of 50, 100, 200 bar and temperature of 40, 60, 80°C to check the experimental set up and mathematical model. The diffusion coefficients calculated by these experiments were compared with the reported values in the literature. Cussler, 1976 and Reid et al.,1977 have found D_{CO_2} in water at 25°C. Comparison of their value, 1.92E-9 m^2/s with my value, 4.86E-9 m^2/s at Temperature of 40°C agrees well with stokes Einstein equation that says the diffusion coefficient increases with the temperature. Also, the results for pressure of 50,100, 200 bar respectively with values of 4.86E-9, 9.6E-9, 8.06E-8 m^2/s show that the diffusion coefficient is increasing with pressure, i.e., the initial concentration of CO_2 in the system and indicate the dependency of diffusion coefficients on concentration. Experiments for porous media all have been done at 100 bar and compared with the experiments for oil. For instance the results of Schoenkirchen oil has the value of 1.5E-8 m^2/s Whereas the same experiment for saturated Berea sandstone at the same condition has the value of 8.03E-10 m^2/s. That shows the D_{CO_2} in porous media has lower value when compared to oil.

3

Kurzfassung

Um die Ausbeute von hochviskosem Schweröl zu erhöhen, wird die Kohlendioxidinjektion angewandt. Dabei hilft CO_2 die Ölmobilität zu erhöhen, indem es durch Mischung mit dem Öl eine niedrigere Viskosität erzielt. Ein besseres Verständnis der Diffusionskoeffizienten von CO_2, D_{CO2}, in porösen Medien, die ein wichtiges Thema bei solchen Ölfeldern ist, ist das Hauptziel meiner Arbeit.

In dieser Arbeit habe ich D_{CO2} in porösen Medien unter Initialleskonditionen über physikalische Experimente analysiert. CO_2-Gas wurde in einen Container/Kernhalter mit Wasser/Öl gesättigten Berea Sandsteinkernen bei Temperatur von 40, 80°C und Druck von 100 bar injiziert.

Der Druck in dem System ändert sich wenn die CO_2-Moleküle in dem porösen Medium zu diffundieren starten. Die Druckabfall über die Zeit ist abhängig von der Diffusionsgeschwindigkeit und von dem Diffusionskoeffizient, deshalb wurde der Druckabfall genau betrachtet und in einer mathematischen Modell definiert, um den Diffusionskoeffizienten zu interpretieren.

Das mathematische Modell wurde durch Fick'schen Gesetz definiert und der Diffusionskoeffizient mit der Hilfe von Druckabfall-Profil berechnet.

Einige Experimente mit Wasser/Brine wurden bei einem Druck von 50, 100, 200 bar und einer Temperatur von 40, 60, 80°C durchgeführt, um das experimentelle und mathematische Modelle zu überprüfen. Die durch diese Experimente berechneten Diffusionskoeffizienten wurden mit den Werten aus den wissenschaftlichen Quellen verglichen. Cussler, 1976 und Reid et al., 1977 haben D_{CO2} im Wasser bei 25°C untesucht. Vergleich ihres Wertes (1.92E-9 m^2/s) mit meinem Wert (4.86E-9 m^2/s) bei einer Temperatur von 40°C stimmt gut mit Stokes Einstein-Gleichung überein. Die Ergebnisse zeigen, dass der Diffusionskoeffizient mit Druck von 50, 100, 200 bar ansteigt und bestätigen die Abhängigkeit des Diffusionskoeffizienten von CO_2 – Konzentration.

Experimente im porösen Medium wurden bei 100 bar durchgeführt und mit den Versuchen in Öl verglichen. Beispielsweise, die Ergebnisse der Schönkirchen Öl haben den Wert von 1.5E-8 m^2/s während die gleichen Versuche bei gleichen Konditionen für gesättigten Berea Sandstein den Wert von 8.03E-10 m^2/s zeigen. Das zeigt, dass die D_{CO2} in porösen Medien niedrigere Werte in vergleich mit Öl hat.

Acknowledgements

I would like to thank my supervisors, Prof. S.K. Matthäi and Dr.Klaus Potsch for their continued support and encouragement.

Table of Contents

6

List of Figures

List of tables

Notation table

Symbol	Meaning	Unit
D	Diffusion coefficient	m²/s
D_{CO_2}	Diffusion coefficient of CO2	m²/s
Deffc	effective diffusivity	m²/s
J	Flux	$mol.s^{-1}.m^{-2}$
c	concentration	$mol.m^{-3}$
X	distance(position)	m
t	time	s
c	average concentration	mol.m-³
c_∞	concentration in unlimited distance	mol.m-³
Z	Compressibility factor	
P	Pressure	bar
Pr	reduced pressure	bar
Pc	critical pressure	bar
Vg	Gas volume	cm³
Vr	reduced volume	cm³
Vc		cm³
T	Temperature	K
Tr	reduced Temperature	K
Tc	critical Temperature	K
µ	chemical potential	
λ	interaction parameter	
φ	fugacity coefficient	%
y	mole fraction	
R	Gas constant	$bar.cm^3.mol^{-1}.K^{-1}$
m	molality of components dissolved in water	mol/kg
k_b	Boltzmann'constant	$J.K^{-1}$
f	friction coefficient of solute	Kg/s
ID	inner diameter	mm
L	Height of liquid column	cm
K	Permeability	md
Por-eff	effective porosity	%
Pv	pore volume	cm3
$V_{co2(aquifer)}$	CO2 volume in aquifer	cm3
N	Number of moles	mol
A	Cross section of the container	cm²
T`	derivative with respect to time	
X``	second derivative with respect to space	

1.Introduction

Cussler, 1976 has his famous experiment for interpreting diffusion coefficient. He examined diffusion coefficients of different gases in gas, liquid and solid. He has also examined D_{CO_2} in water at 25°C using two bulbs containing water or CO_2 gas that were connected through capillary tube to each other. His experiment led to D_{CO_2} of 1.92E-9 m^2/s in water, (Cussler, 1976; Reid et al.,1977). This value agrees well with my value of 4.86E-9 m^2/s at T 40°C according to Stokes Einstein equation that explains direct relation of temperature and diffusion container meaning that the diffusion coefficient increases with temperature.

However, Grogan, et al.,1988 estimated the D_{CO_2} in water at high pressure from Stokes-Einstein equation. But Having experiments at reservoir conditions would be beneficial to determine a relationship between high-pressure and atmospheric-pressure data. Difficulty in the laboratory for experimental set up is the reason of having only few experimental studies of D_{CO_2} at high-pressure. Even no D_{CO_2} in water is available at reservoir conditions in the literature.

Grogan, et al.,1988 also measured diffusion coefficients for CO_2 in oil at 25°C and pressure of 52 bar .The result is 2E-9 m^2/s.

Unatrakarn, et al., 2011 has experimental values of 3.4-6.8E-8 for D_{CO_2} in oil at 30-55° C and 24-26 bar and 1.8-2.41E-8 in oil saturated porous media at 30-55° C and 28-32 bar with viscosity of 21,285-8,154 cP. His description for that was tortuous pathways in the porous system.

Yang and Gu, 2006 has set up several experiments for heavy oil with viscosity from 800-23 Pas at temperature of 20-25°C and pressure of 2-6 MPa. Their evaluation results for the D_{CO_2} into Crude oil is 0.12-0.55 E-9 m^2/s.

The mass transfer of CO_2 into water has been studied by Farajzadeh, et al., 2007 at different pressures and a constant temperature. The results show the transfer rate is initially much larger than expected from a diffusion process alone. He has a value in the range of 1.95-3.5E-9 for the D_{CO_2} into water.

Renner, 1988 has been developed a method for measuring molecular D_{CO_2} in consolidated porous media saturated with NaCL at pressure of 15-58 bar and temperature of 38. He achieved D_{CO_2} in the range of 3-7E-9 m^2/s.

Darvish, et al., 2006 has also experimental research of CO_2 injection into fractured cores at reservoir conditions of 300 bar and 130° C. They used extended Sigmund correlation for evaluating D_{co_2}. Their value is 1.38E-11 m^2/s.

Fenglan, et al., 2011 has developed laboratory method to measure the diffusion coefficients of CO_2 in the porous medium under high pressure and temperature. It is found that the diffusion coefficients grow as the pressure increases. Their results vary from 0.66 E-9 to 1.22E-9 m^2/s for the permeability of 0.49-0.84 md, a porosity in the range of 32.85-35.94% and condition of 1371-5117 MPa. Assuming different boundary conditions identify their work from each other. Almost all have a constant gas compressibility factor during the experiment.

An increase in the saturation of the oil phase due to swelling and a significant reduction in the oil viscosity are the main reasons why CO_2 injection can be used to enhance oil recovery from heavy oil reservoirs. The application process depends highly on each reservoir characteristics and reservoir management is the most important issue in this process.

Dissolution of CO_2 in the reservoir fluids is controlled by convection and diffusion processes. Diffusion rates can affect gas/oil displacement and diffusion evaluation therefore, become crucial for performance prediction and is needed also to determine correct amount of CO_2 required for the injection processes.

This thesis evaluates D_{co_2} at late time assuming that the diffusion is the only mechanism of the mass transfer. The main objective of this work was setting up of an experiment where CO_2 gas was injected into water/oil saturated Berea sandstones to measure the pressure decline as the CO_2 gas dissolves into the water/oil. D_{co_2} are subsequently interpreted from the measured pressure decline due to the dissolution and diffusion of gas. A mathematical model using Ficks law has been developed to estimate the mass transfer by diffusion whereas three models were defined for pressure decline.

Review of the literature, results in following main issues:

I. Assuming gas compressibility factor as a constant parameter while it changes with changing pressure in the system.

As the mathematical model in the next section and Figure 1, calculated with OMV internal program, show that the gas compressibility is changing with the time and supposing constant compressibility for gas, in mass transfer of CO_2 into heavy oils (Zhang, et al., 2000) is not a correct idea.
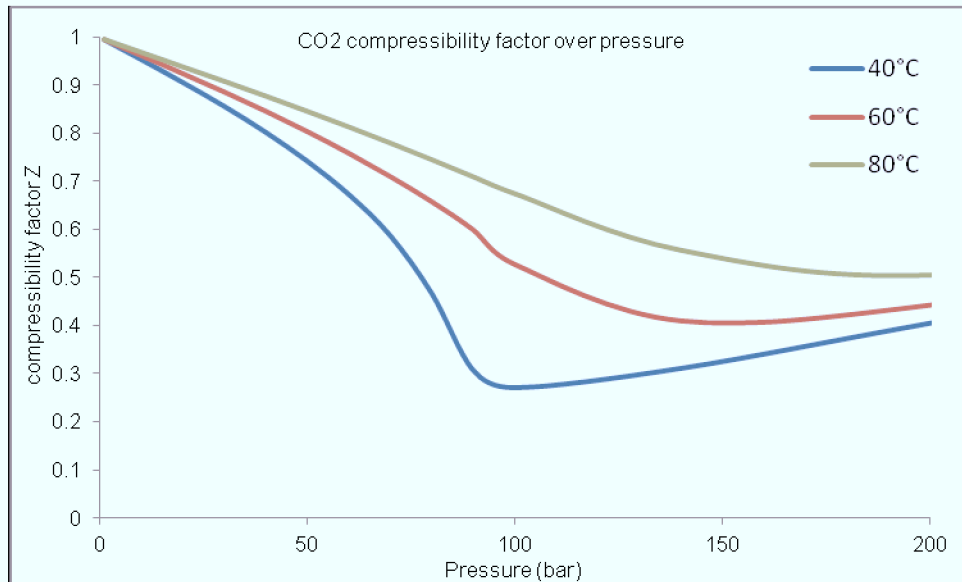
Figure 1: CO_2 compressibility factor as a function of pressure.

II.   Definition of the correct initial and boundary conditions for the mathematical concept is very tricky and not easy to handle it correctly.

This thesis, will focus in these issues and will address the solution by defining a new mathematical model using fick's law combined with gas law by giving new ideas for the experimental setup.

2. Methodology

Cussler, 1976 has run an experiment to interpret the diffusion coefficient. His experiment has two large bulbs initially containing different gases connected by a long thin capillary. The bulbs are at constant T, P and equal volumes. One bulb contains CO_2 and another one has the same amount of N_2, he measured the concentration of CO_2 in the bulb of N_2
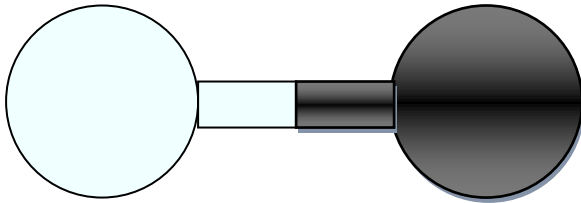
Figure 2: Cussler's experimental set up

In Figure 2, each colour represents one of the gases and as the schematic of the experiment shows the same amounts of the gases were used. He assumed that the flux (J) is proportional to the gas concentration and recognised that flux and capillary's length have inverse relation:

$$J = D\frac{concentration difference}{length of capillary}$$

Introduction of D in the equation remember us a model for diffusion that called Fick's first law:

$$J = -D(\frac{\partial c}{\partial x})$$

D is diffusion coefficient in dimensions of *length²/time* , $m^2.s^{-1}$

and

J stands for the flux in dimensions of *amount of substance.length-².time⁻¹* , $mol.m^{-2}s^{-1}$

c: the concentration in dimensions of *amount of substance·length⁻³* , $mol.m^{-3}$

x : the position, length (*m).*

Later on, he identifies that the concentration varies linearly with time and therefore implies Ficks second law:

$$\frac{\partial c}{\partial t} = D\nabla^2 c$$

where t is the time(s).

Using the Fick's first law and the mass balance it can be derived in one dimension as following equations:

$$\frac{\partial c}{\partial t} = -\frac{\partial}{\partial x}J = \frac{\partial}{\partial x}(D\frac{\partial c}{\partial x})$$

$$\frac{\partial c}{\partial t} = D(\frac{\partial^2 c}{\partial x^2})$$

Fick in his second law shows non steady diffusion in which the concentration varies with the time.

Cussler developed the analytical solution for this partial differential equation as:

$$\frac{c_0 - \bar{c}}{c_\infty - \bar{c}} = erf(\frac{x}{2\sqrt{Dt}})$$

The effective diffusion coefficient in inhomogeneous porous media can be found using next equation

$$Deff = validfraction(\frac{D}{\tau})$$

But as I used homogeneous Berea sandstone in my experiments, there was no need for applying this equation:

As much as diffusivity, gas solubility is also important in CO2 injections that is a function of composition, pressure and temperature in aqueous solutions.

Duan, 2003 has valuable research to interpret the solubility of CO_2 in pure water and brine:

Firstfully he developed equation of state for CO_2 and says Ln φ_{CO2} can be calculated from the EOS for pure CO_2 (Duan et al., 1992b).

$$Z = \frac{P_r V_r}{T_r} = 1 + \frac{a_1 + a_2/T_r^2 + a_3/T_r^3}{V_r} + \frac{a_4 + a_5/T_r^2 + a_6/T_r^3}{V_r^2} + \frac{a_7 + a_8/T_r^2 + a_9/T_r^3}{V_r^4} + \frac{a_{10} + a_{11}/T_r^2 + a_{12}/T_r^3}{V_r^5} + \frac{a_{13}}{T_r^3 V_r^2}(a_{14} + \frac{a_{15}}{V_r^2})\exp(-\frac{a_{15}}{V_r^2})$$

Values of a are presented by Duan et al. (1992a) in the Table 1.

Table 1: Values of a, By Duan et al. (1992a)

a_1	$8.99288497e-2$
a_2	$-4.94783127e-1$
a_3	$4.77922245e-2$
a_4	$1.03808883e-2$
a_5	$-2.82516861e-2$
a_6	$9.49887563e-2$
a_7	$5.20600880e-4$
a_8	$-2.93540971e-4$
a_9	$-1.77265112e-3$
a_{10}	$-2.51101973e-5$
a_{11}	$8.93353441e-5$
a_{12}	$7.88998563e-5$
a_{13}	$-1.66727022e-2$
a_{14}	$1.39800000e+0$
a_{15}	$2.96000000e-2$

$$\ln\varphi(T,P) = Z - 1 - \ln Z + \frac{a_1 + a_2/T_r^2 + a_3/T_r^3}{V_r} + \frac{a_4 + a_5/T_r^2 + a_6/T_r^3}{2V_r^2} + \frac{a_7 + a_8/T_r^2 + a_9/T_r^3}{4V_r^4} + \frac{a_{10} + a_{11}/T_r^2 + a_{12}/T_r^3}{5V_r^5} + \frac{a_{13}}{2T_r^3 a_{15}}(a_{14} + 1 - (a_{14} + 1 + \frac{a_{15}}{V_r^2})\exp(-\frac{a_{15}}{V_r^2}))$$

This model is extended to predict CO_2 solubility.Where

T is absolute temperature in Kelvin

P: total pressure of CO_2-brine system in bar

y: mole fraction of CO_2 in vapor phase

R: universal gas constant; = 0.08314467 bar L mol^{-1} K^{-1}

m: molality of CO_2 or salts in the liquid phase

u: fugacity coefficient

Where P_r, T_r, V_r are reduced pressure, reduced temperature, and reduced volume, respectively and P_c, T_c are the critical pressure, critical temperature and $V_c = RT_c/p_c$

His model for calculating the solubility has the following form

$$\ln m_{CO2} = \ln y_{CO2}\phi_{CO2}P - \mu_{CO2}/RT - 2\lambda_{CO2-Na}(m_{Na} + m_k + 2m_{Ca} + 2m_{Mg}) - \zeta_{CO2-Na-Cl}m_{Cl}(m_{Na} + m_k + m_{Mg} + m_{Ca}) + 0.07m_{SO4} \qquad (1)$$

This model later on was used to calculate the solubility of CO_2.

Dissolution of the CO_2 into liquid phase leads to an increase in liquid volume and changing of the liquid level in the container that is called shrinkage or swelling of the liquid phase, but since my CO_2/Liquid value is very law which means I used very small volume of CO_2 gas in a quite small containers this shrinkage of liquid volume could be ignored respect to my mathematical model.

15

Diffusion coefficient depends on the concentration, pressure, viscosity of the solvent and temperature, the last one has a direct relation with the diffusion coefficient according to the Stokes-Einstein relation.

$$D = k_b \frac{T}{f}$$

where

k_b: Boltzmann's constant

f: friction coefficient of the solute(CO_2)

Now imagine my experimental set up as following, where the CO2 is injected on top of saturated Berea sandstone and left for some time to monitor the pressure decline in the closed system with constant temperature. The concentration of CO_2 in vertical position and pressure decline are presented in the Figure 3.
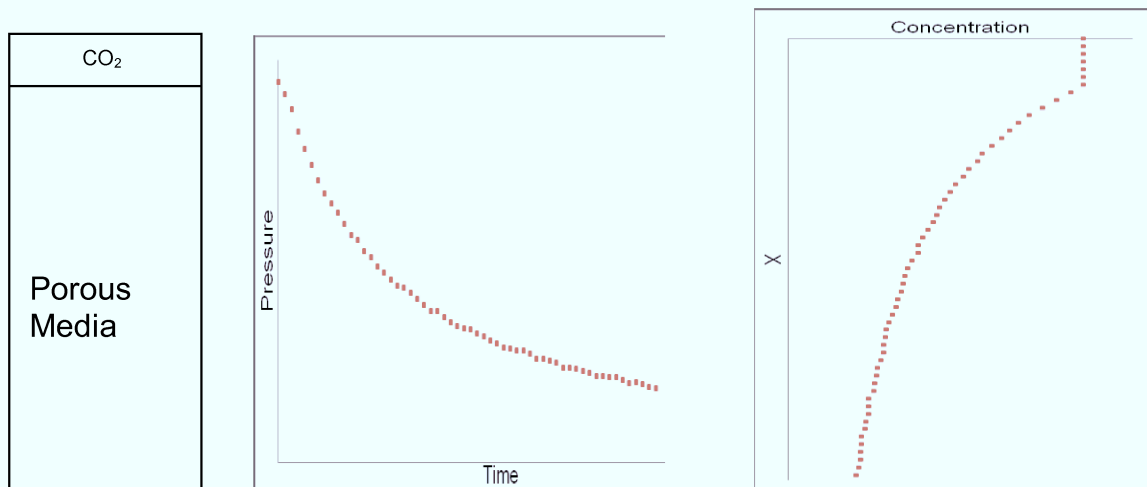
Figure 3: Schematic of the container containing CO_2, Porous media and its pressure decline and concentration profile

2.1 Experimental set up

All the experiments have been done in OMV Laboratory for Exploration and Production with the goal of measuring the pressure decline in the container, containing CO_2-porous media (saturated with water/oil), CO_2-water, CO_2-oil, CO_2-brine (Figure 4), during the dissolving of the CO_2 in reservoir fluid to determine the D_{CO_2} in liquids whereas CO_2 was in super critical phase for the all experiments.
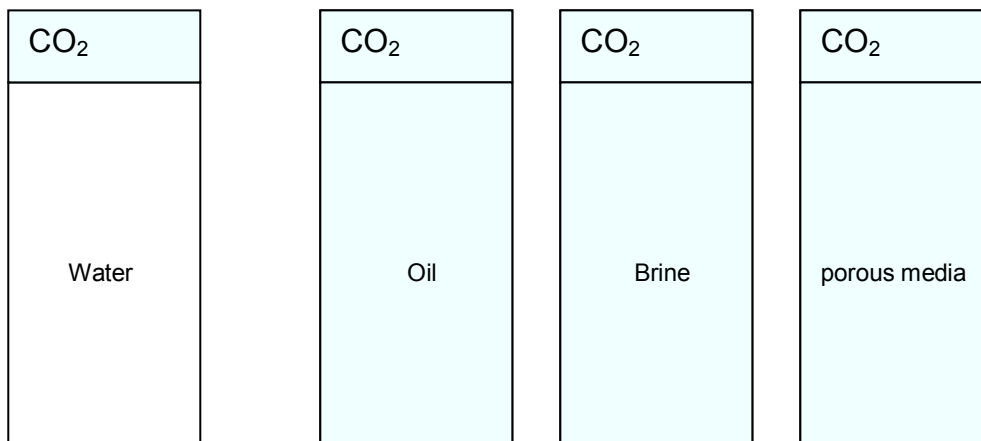
Figure 4: CO2 in contact with water, oil, brine, porous media.

Zhang, et al., 2000 and Farajzadeh, et al., 2007 set up an experiment for interpreting D_{CO2}. During experimental part of my work in the laboratory I used also similar set up, but with some differences. For instance they had gas in the cell and afterward let the oil to enter the system whereas I had my porous media in container and then the CO2 gas was injected into the container.
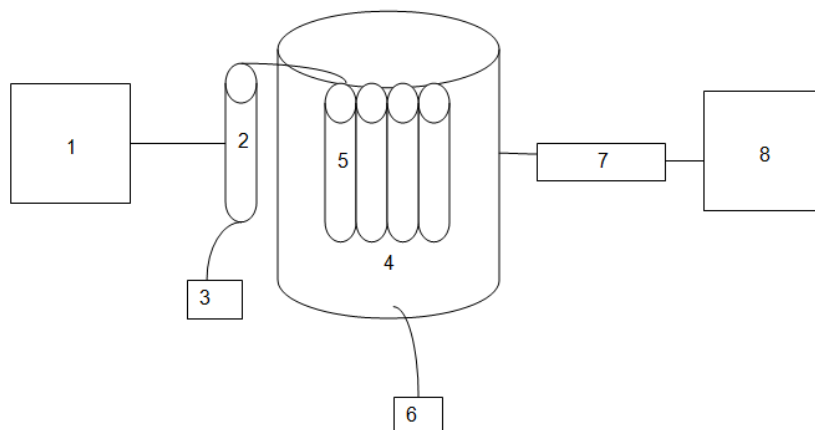
Figure 5: Schematic diagram of experimental set up

Four containers (Part 5 in Figure 5) have been placed in a liquid bath (Part 4 in Figure 5) to maintain the temperature with thermostat at the desired temperature. Thirty-minute waiting time was respected for liquid in containers coming into thermal equilibrium with the liquid bath. Top of the containers were connected to a high-pressure gas cylinder (Part 2) and CO_2 gas was injected in certain amount into the container/core holder by the constant rate. A computer was also connected to gas cylinder to manage the injected gas volume (Part1). A pressure transducer connected to the containers (Part 7) to measure the pressure change inside the container during the experiment. Part 8 of Figure 5 is a computer that monitors the pressure decline in each container and the temperature of the liquid bath and gas cylinder both were constant and were measured by the thermostat. Part 3 and 6 are respectively thermostats for gas cylinder and liquid bath. During the operation, sides of containers were closed, each container was connected to the separate pressure sensor.

Dimensions of the container and core holder are presented in the Table 2, 3.

Table 2: Dimensions of container

Containers		
ID	28	mm
L	300	mm
Weight	1900	g
volume	184.63	cm3

Table 3: Dimensions of core holder

	ID	length	
coreholder	32.05	100	mm

Experiments include experiments with water, brine, oil and water/oil saturated cores. Oil samples were from Vienna basin and Berea sandstone was used as porous media in the experiment. Figure 6 shows some pictures from the experimental set up.

A

B

C
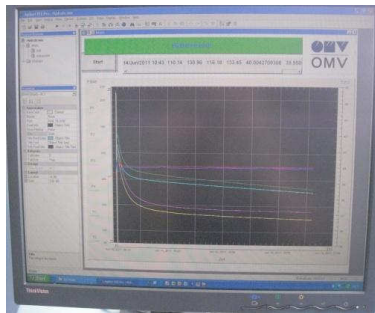
D

E

Figure 6: Pictures of experimental set up
A) Thermostat for the gas line B) Thermostat for the thermal bath C) Schematic of the gas cylinder and PC to control pressure and thermostat D) Pumping line into containers E) Recording data by the PC

The variation of pressure for each experiment was recorded as a function of time while gas phase diffused into the liquid phase. A significant change of pressure in the gas phase at the beginning of the experiment was observed which indicates that the mass transfer rate of gas was changing with time.

Some primary preparing works and necessary measurements have been done as following:

Since we deal with saline aquifers in reality, we tried to do some experiments with salted water. For this, salt was added into the distilled water to obtain brine as like as

formation water. Oil density and oil gravity have influence on the diffusivity therefore, different types of oil were used. The oil samples were collected from different oil fields of the Vienna basin.

Berea core samples (Figure 7A) were prepared in the same size and similar rock properties to use as porous media and afterward the core data like length, diameter, weight, permeability, matrix volume and bulk volume were measured. Figure 7 shows measuring of permeability, matrix volume, bulk volume of the cores to calculate the effective porosity.

A

B

C
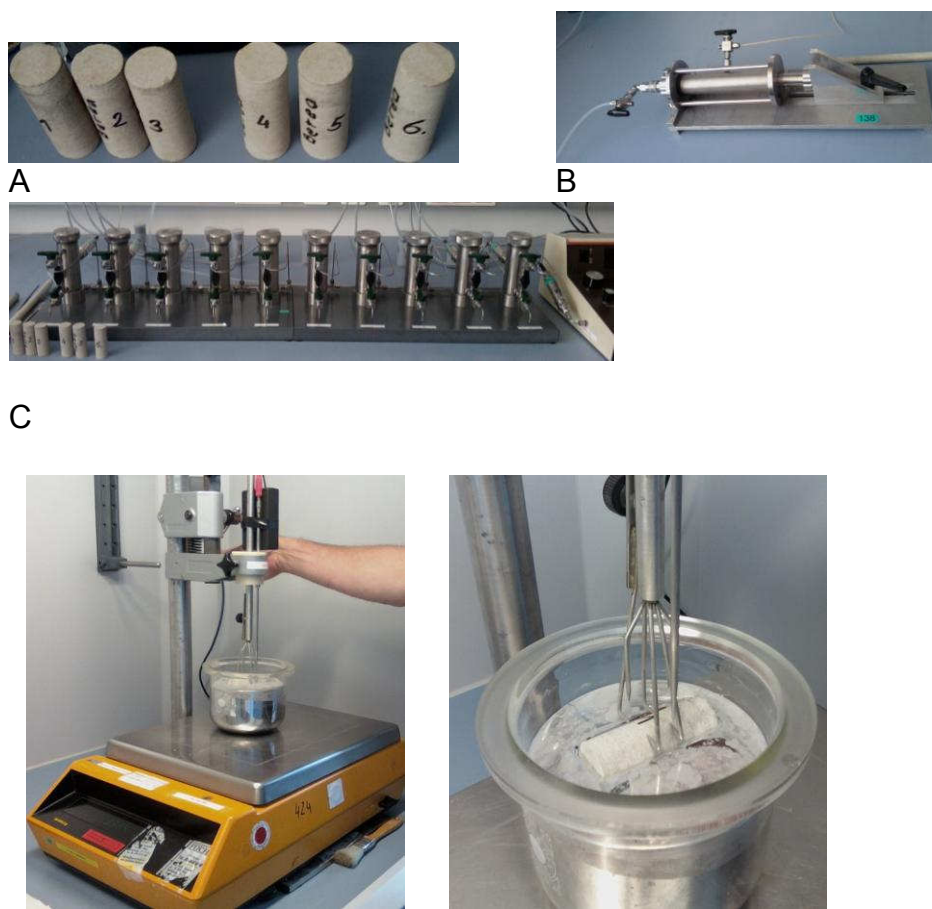
D

Figure 7: Preparing for the experiment
A) Berea cores B) Measuring permeability C) Measuring matrix volume of core D) Measuring Bulk volume of core

Part A of Figure 7 presents prepared Berea sandstones. Figure B shows a core holder containing core of Berea sandstone to measure its permeability. In figure 7C, the Berea sandstone cores were placed in core holders to measure matrix volume for evaluating porosity of cores. In figure 7D, bulk volume of the cores was measured,

20

the used liquid for this purpose is mercury. Porosity of the cores was evaluated with the helium porosity-meter and the important information of cores are presented in the table 4.

Table 4: Data of core samples

Length	6.977	cm
Diameter	2.530	cm
Weight	73.765	gr
Vol	35.073	cm3
Matrix-Vol	27.630	cm3
Por-eff	21.223	%
Density	2.670	gr/cm3
Pv	7.443	cm3
K	230.901	md

For the experiments in the presence of porous media, the Berea cores were left in the liquid bath overnight (Figure 8) and evacuated to push the air out from the pores, thereby sandstone has been saturated with water/oil, and afterwards placed in containers/core holders and pour some water up to height of cores.

Figure 8: Saturation of the Berea sand stone with water.

For the water experiments, some containers have been filled with glass tubes in it. To see influence of the convection at beginning of the experiment. Pressure profiles show the reduced convection effect in the experiments with the glasses.

Experiments were carried out in several temperatures of 40, 60, and 80°C and pressures of 50, 100, 200 bar for five different salinity of water 1, 2, 5, 10, and 20 with KCL and four different types of oil (Table 5) and compared with similar data in the literature.

Table 5: Summary of all experiments

T	P	brine/oil	container	coreholder	berea
40	50	water/brine1,2,5,10,20%	-		
40	100	water/brine1,2,5,10,20%	-		
40	200	water/brine1,2,5,10,20%	-		
60	100	water/brine5,10,20%	-		
80	100	water/brine5,10,20%	-		
40	100	Gasoil-Stockerau		-	
40	100	Gasoil-Stockerau		-	-
40	100	water-Schönkirchen-Hochleiten		-	-
40	100	water		-	
80	100	water-Schönkirchen-Hochleiten		-	-
80	100	water		-	
40	100	water	-		-
40	100	Gasöl-Schönkirchen-Hochleiten-Stockerau	-		
80	100	Gasöl-Schönkirchen-Hochleiten-Stockerau	-		

2.2 Mathematical principle

The way to know D_{CO_2} in brine and oils was to fill the empty space above a certain amount of water/oil that is contained in a pressurized container. When CO_2 dissolved in the liquid phase, the pressure in the gas cap drops. Therefore, the main data to be recorded was the pressure in the gas cap as a function of time.

Since the whole volume of the container is constant, increase in liquid volume due to dissolution of the gas in it leads to decrease in gas volume, but I will work with the assumption that the liquid volume remains constant because as I mentioned beforehand, my container with 30 cm length and 2.8 cm diameter is a relatively small container and the relation of the used CO_2 gas to liquid phase was very small which leads to really small ignorable volume change $V_{CO_2(aquifer)}$ in both phases. Starting point of the calculation is the equation 2 meaning the gas law

$$p(t) \cdot V_g = N(t) \cdot Z \cdot R \cdot T \tag{2}$$

p, Vg, N, R, T, t, Z stand respectively for pressure (bar), volume (cm^3), number of moles (mol), gas constant ($bar.cm^3.mol^{-1}.K^{-1}$), temperature (Kelvin), time(s) and gas compressibility factor. By the way, the value of gas constant is R=83.14472 $bar.cm^3.mol^{-1}.K^{-1}$.

In the liquid phase we have two equations, firstly the conservation of mass, Equation 3, and second them momentum equation that is Fick's law, Equation 4 that links the flux with the gradient of the concentration

$$\frac{\partial c^*}{\partial t^*} + \frac{\partial J^*}{\partial x^*} = 0 \tag{3}$$

$$\tau \frac{\partial J^*}{\partial t^*} + J^* = -D \frac{\partial c^*}{\partial x^*} \tag{4}$$

With **c** for concentration ($mol.cm^{-3}$), **J** for flux ($mol.s^{-1}.cm^{-2}$), **D** for diffusion coefficient ($cm^2.s^{-1}$)

The aster denotes that the quantities still have physical dimensions that make difficulties in boundary conditions. Therefore, dimensionless equation is suggested here to obtain flux dependent diffusion coefficient instead of concentration dependent. That requires reference quantities of

23

$$x_{ref} = L$$
$$t_{ref} = L^2 / D$$
$$c_{ref} = \frac{N_0 - N_\infty}{L.A}$$

L for height of liquid column (cm), **A** for cross section of the container (cm²)

The subscript 0 and ∞ refer to the initial and final stage of the process. After introducing these constants the equations 3, 4 take the form equation 5, 6:

$$\frac{\partial c}{\partial t} + \frac{\partial J}{\partial x} = 0 \tag{5}$$

$$\varepsilon \frac{\partial J}{\partial t} + J = -\frac{\partial c}{\partial x}, \quad \varepsilon = \tau.D / L^2 \tag{6}$$

Eliminating the concentration we get equation 7

$$\varepsilon \frac{\partial^2 J}{\partial t^2} + \frac{\partial J}{\partial t} = \frac{\partial^2 J}{\partial x^2}, \tag{7}$$

For this partial differential equation initial and boundary conditions have to be formulated. Using initial condition of

$$t = 0, x > 0: \quad c = c_0 \quad \text{or} \quad J = 0$$

And two boundary conditions of

$$x = 0, t \geq 0: \quad J = J_0(t)$$
$$x = 1, t \geq 0: \quad J = 0$$

The normalized flux into the liquid phase using equation 2 is found in the form of

$$J(x = 0, t) = \frac{1}{A} \frac{dN(t)}{dt} = \frac{V_g}{ART} \frac{d(p/Z)}{dt}$$

This flux is the one at the interface between gas and liquid. We concentrate now on the case with $\varepsilon = 0$. The solution is found by the separation of variables in the form of equation 8

$$J(x,t) = X(x)T(t) \tag{8}$$

Inserting this expression, Equation 8, into equation 7 and dividing it by *X.T* we get

$$\frac{\dot{T}}{T} = \frac{X''}{X} = -k^2$$

The point symbolizes the derivative with respect to time, the prime the one with respect to space. Since the two sides of the equation depend on different variables, they can only be equal to a constant. The solutions are obtained through damped wave equation and presented

24

$$T \propto \exp(-k^2 t) \quad \text{and} \quad X = A\cos kx + B\sin kx$$

The boundary conditions help us find the constants *A=1* and *B=0* and *k* has to be equal to *k=(2n-1).π/2*. Thus the solution takes the form

$$J(x,t) = \sum_n A_n \cos(2n-1)\frac{\pi}{2} x \cdot \exp\left(-\left((2n-1)\frac{\pi}{2}\right)^2 t\right)$$

The constants *A_n* are determined through the boundary condition.

$$J(x=0,t) = J_0(t) = \sum_n A_n \cdot \exp\left(-k_n^2 t\right) \quad \text{with} \quad k_n = (2n-1)\frac{\pi}{2} \tag{9}$$

The concentration *c(x,t)* results from integrating equation 5

$$c(x,t) = \int J \, dx + c_\infty$$

A plot of equation 9 reveals that for the beginning of the process only the first term (n=1) plays a significant role

$$J(x=0,t) = J_0(t) = A_1 \cdot \exp\left(-k_1^2 t\right) \quad \text{with} \quad k_1 = \frac{\pi}{2} \quad \text{or}$$

$$\ln J = \ln A_1 - \frac{\pi^2}{4}\frac{t^*}{t_{ref}} = \ln A_1 - \frac{\pi^2 D}{4 \cdot L^2} t^* = \ln A_1 - bt^*, \quad \text{with} \quad b = \frac{\pi^2 D}{4 \cdot L^2}$$

As I already mentioned in the introduction part, this model deals with relation of D_{CO_2} with the flux of the gas into the liquid phase. The constant b is then the slope of the flux in a semi-log plot. Having the slope determined one can calculate the diffusivity by:

$$D = b\left(\frac{2L}{\pi}\right)^2$$

$$(10)$$

3. Results and Interpretation

Before to go deeper in diffusivity interpretation, I would present CO_2 solubility in water using Duan, 2003 model for calculating the solubility, Equation 1 that presented with detail in methodology section. The results of CO_2 solubility in water at 40°C was calculated by Duan model in the Table 6.

Table 6: Solubility as a function of pressure.

P(bar)	solubility	
50	1	mol/kg
100	1.3	mol/kg
200	1.5	mol/kg

As the Figure 9 shows the solubility of CO_2 in water increases with the pressure.
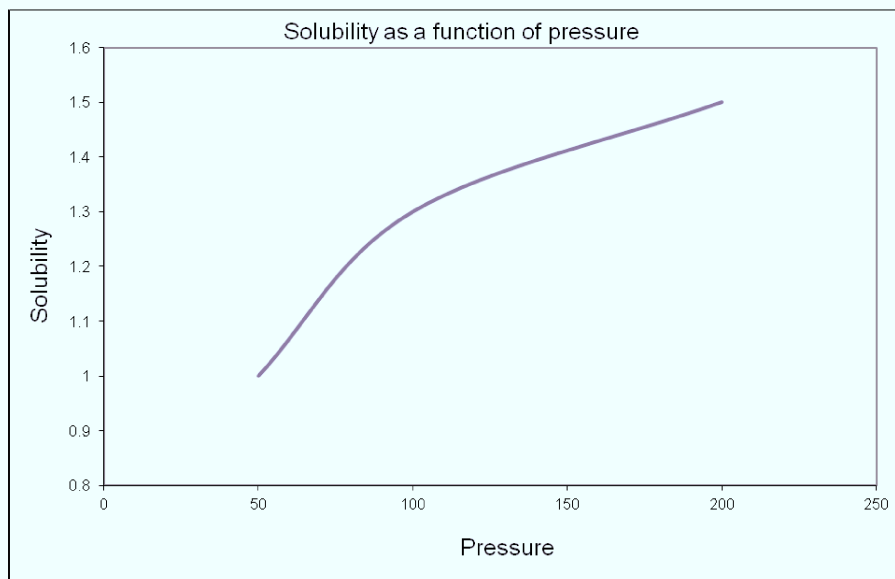
Figure 9: Solubility as a function of pressure

26

3.1 Pressure plots

In the following pages the pressure decline as a function of time for water and brine experiments is compared for glasses and without glasses cases.
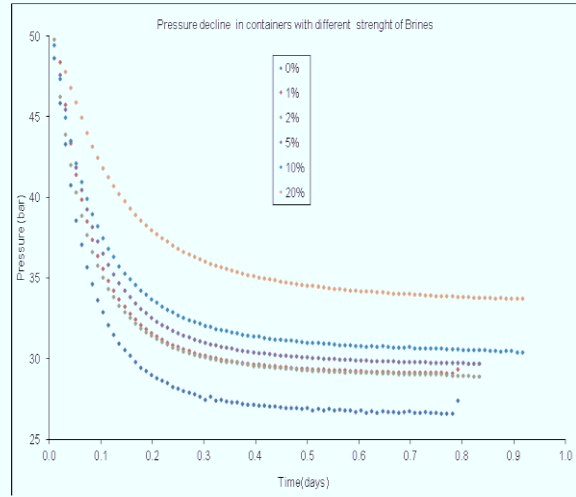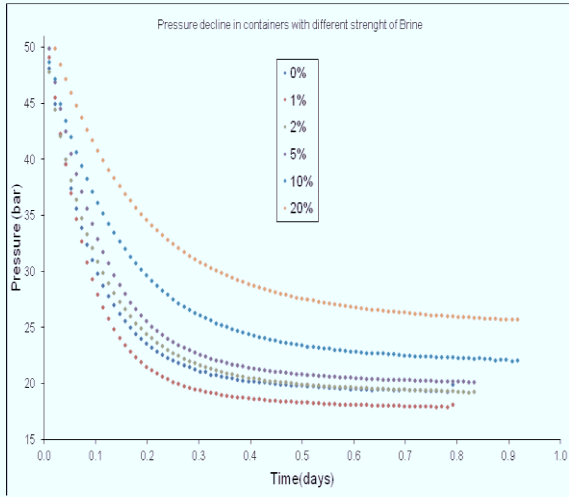
A
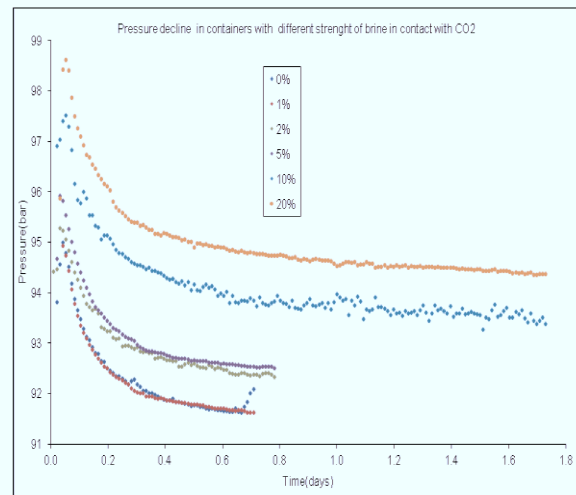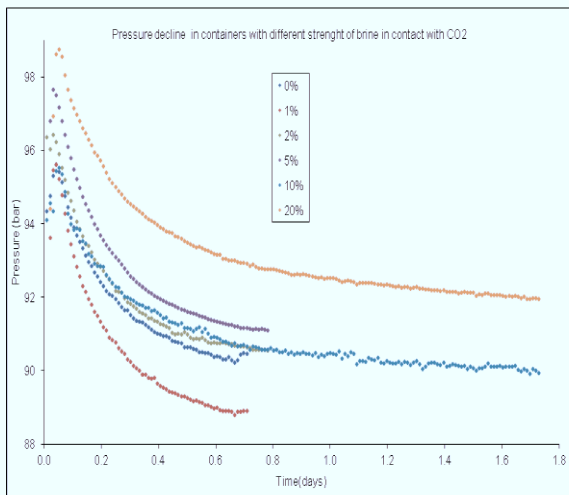
B
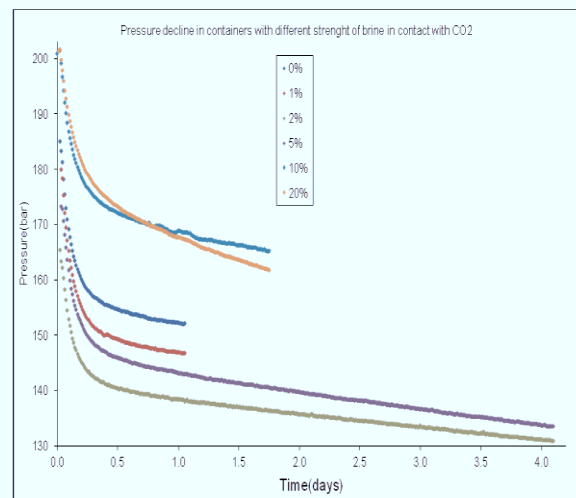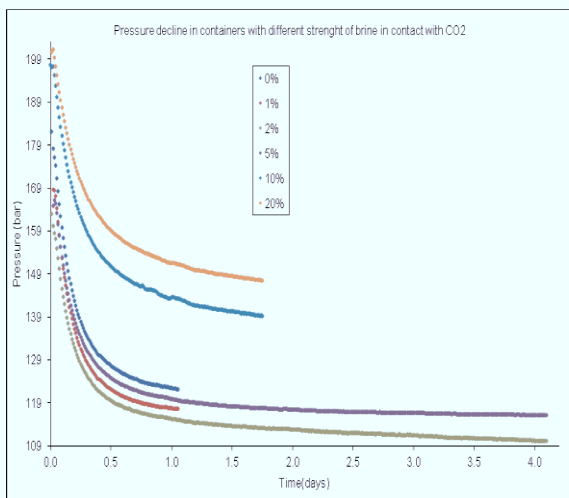
C
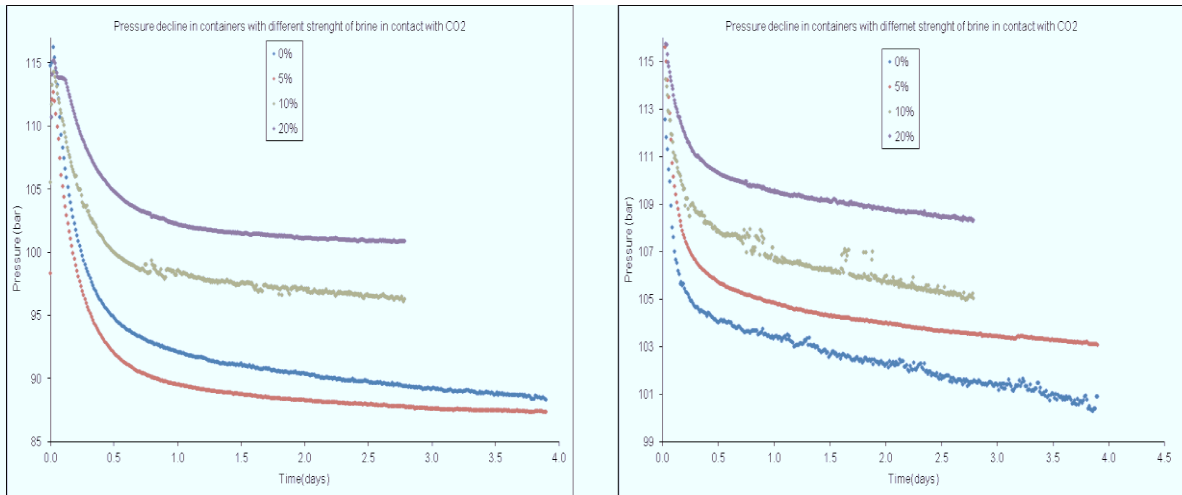
D
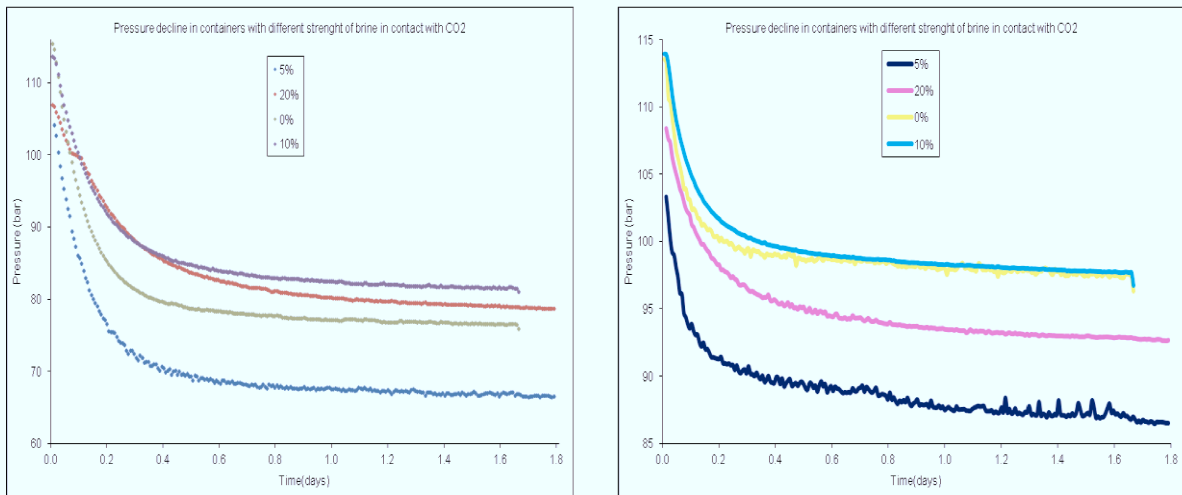
E

Figure 10: Pressure decline in containers with different strength of brine in contact with CO2 without glasses on the left side and with glasses on the right side
A) at 40°C & 50 bar B) at 40°C & 100 bar C) at 40°C & 200 bar D) at 60°C & 100 bar
e) at 80°C & 100 bar

Part A of Figure 10 is presenting the experiment at 40°C& 50 bar, comparing these two cases, one with glasses another one without glasses, pressure decline in right order of salinity in containers with glasses shows reduction of convection effects. In other hand, less pressure decline in higher salinity brines expresses the less solution of CO_2 in brine.

Part B of Figure 10 implies also a good performance of using glasses with showing correct order of pressure decline with salinity, i.e., more pressure decline with salinity. Almost the same pressure decline for 0,1 and 2,5 brines is due to closed salinity and influence of higher initial pressure (100 bar).

Comparing pressure declines in 10C with 200 bar initial pressure, we notice that using glasses did not help for reduction of convection effect as the declines do not follow regular pattern with salinity.

Part D shows less pressure drop in brine with higher salinity that is more logical than declines in containers without glasses, this ordered plot shows importance of using glasses to reduce the convection effects.

Part E shows although less pressure drop in brine with higher salinity is expected, but it is not presented in the pressure plots. The conclusion for using glasses in container would be:

At higher temperatures convection in liquid phase enhances the mass transfer rate more efficiently. In general, comparing experiments using glasses and experiments without glasses, we notice that using glasses helped in reduction convection effects in lower pressure and temperature, while it did not help neither in higher pressure of 200 bar nor in high temperature of 80°C.
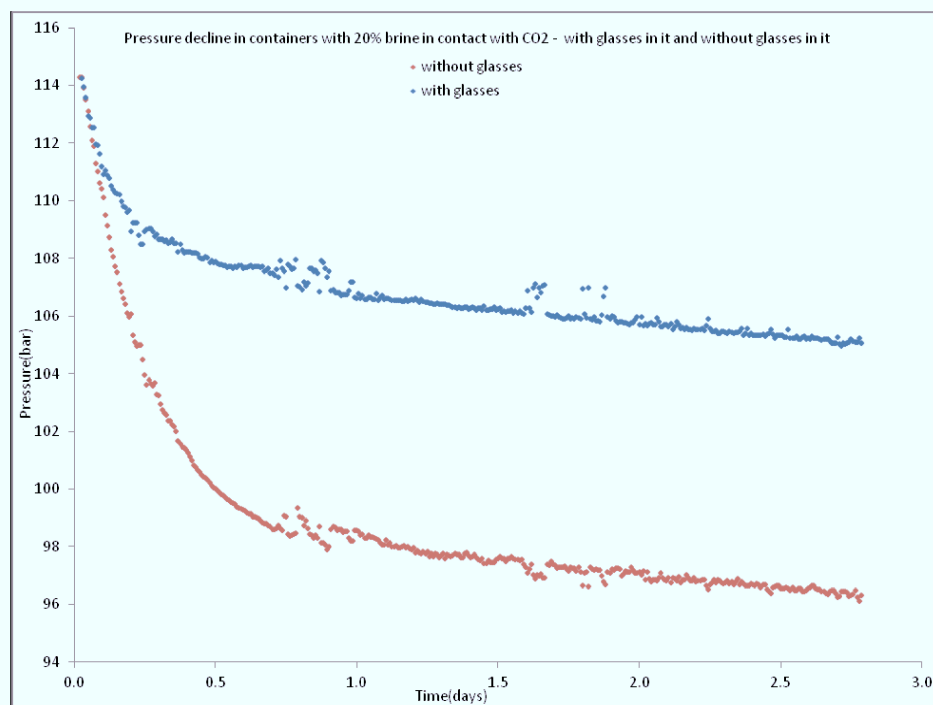
Figure 11: Brine of 20% in contact with CO2 at 60°C &100 bar

29

Attention to Figure 11 we notice that, due to the use of the containers of the same size, using glasses leads to less water using which results in less pressure reduction and at the same time, less CO_2 mass transfer into the brine, results in reduced convection. But it should be considered that the tube glasses do not totally remove the convection effect, but instead they only reduce it.

This section remained that the dissolution of CO_2 in brine depends on brine salinity, pressure and temperature.

3.2   Experiments with different oil types (Vienna basin Austria)

CO_2 was brought into contact with some Oil samples separately such as Schoenkirchen, Gasoil, Stockerau Ost and Hochleiten.

All of experiments have been performed at 100 bar, either in container or core holder, which was smaller than container.

The densities of oil samples are shown in the table 7.

Table 7: Oil density

Gasoil	0.8382	g/cm³
Schönkirchen	0.9337	g/cm³
Hochleiten	0.9333	g/cm³
Stockerau ost	0.7230	g/cm³

In reference to previous thesis, Xia Jing, Schönkirchen and Hochleiten are characterized as heavy oil.

Some of experiments did not reach the required time to be evaluated due to the time limit or gas leakage during the experiment.

The monitored pressure declines in container/core holder are shown in the next pages.

Demo Version, http://www.verydoc.com and http://www.verypdf.com

A   B
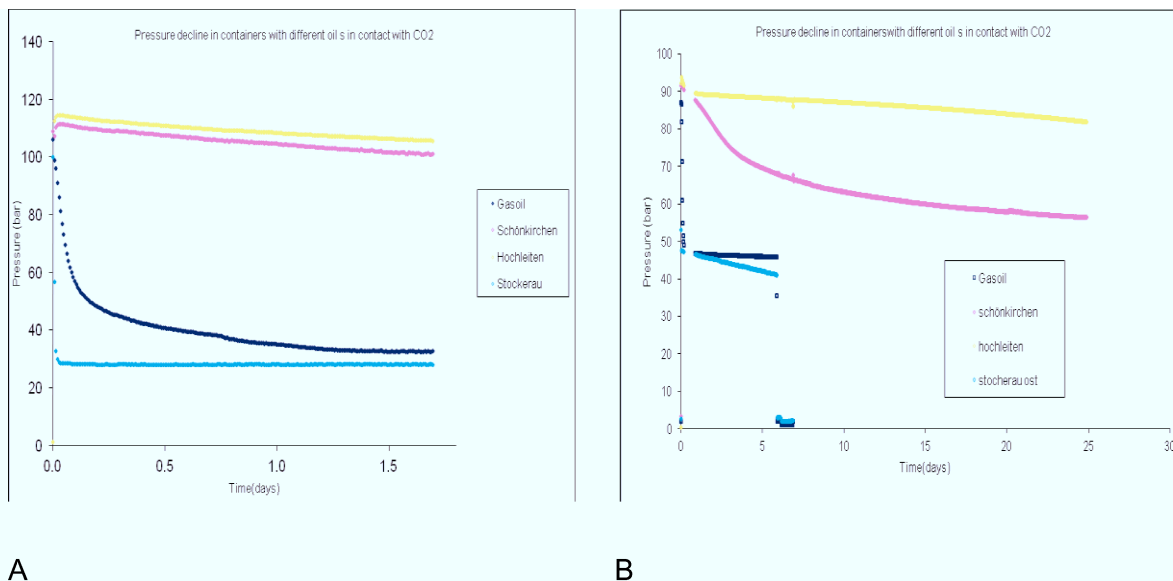
Figure 12: Different oils in contact with CO2 at 80°C &100 bar, on the left side and 40°C, on the right side

In this experiment (Figure 12A), due to some difficulties in setting the experiment, we started from a bit upper pressure than the desired initial pressure.

As the density table shows, Hochleiten and Schönkirchen are denser and their pressure decline is slower than other two oil types.

The pressure drops during the dissolution of CO_2 in Stockerau and Gasoil were very rapid at 80°C & 100 bar, and the pressure did not decrease largely any more. This kind of pressure slump could be caused by a relative high dissolution rate of CO_2 in this kind of oils.

To reach equilibrium in diffusion process in denser oils, we increased the pressure observation time in this case.

Comparing two previous experiments we figure out that in both temperatures, Hochleiten is less miscible than others and Stockerau is the most miscible one, followed by Gasoil and Schönkirchen which are respectively second and third miscible oil samples.

Although Stockerau oil sample at 80°C reached approximately 30 bar after one and half day, but it was still around 50 bar at 40°C at the same time. Hence, we notice that CO_2 become less miscible with Stockerau in lower temperature.

The continuity of the pressure decline in Schönkirchen and Hochleiten after 26 days can still be interpreted as leaking of the CO_2 from the container.

3.3 Container & Core holder

Experiments in container shows small amount of gas leakage from the container therefore some of the experiments have been repeated with using core holder instead of using container and important information are presented in the Table 8 while the experiment results are presented in the Figure 13.

Table 8: Different amounts of oil and CO_2 used in container/core holder(water)

	container	core holder	
H2O	156.98	60.19	g
CO2	26.87	57.75	cm3
saturated cores			
H2O	51.59	10.07	g
CO2	69.61	29.7	cm3
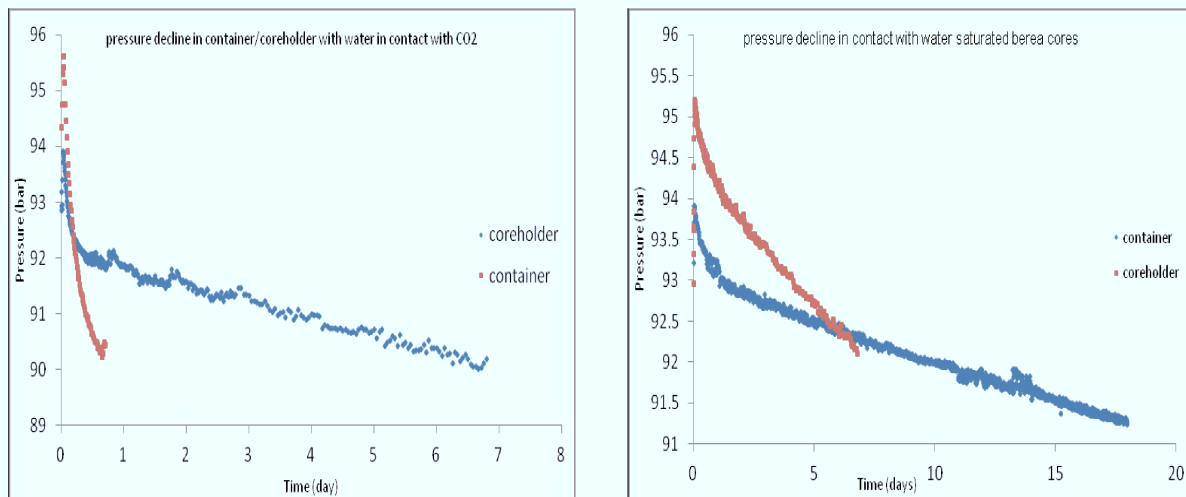
A   B

Figure 13: Water in contact with CO2 at 40°C &100 bar, on the left side and water saturated Berea cores, on the right side

Pressure decline after one day up to 90 bar (Figure 13A) expresses more rapid pressure decline in the container. Considering the amount of used gas and liquid emphases the accuracy of the experiment in container. In general, using less gas rather than liquid will lead to more accurate experiments.

32

In Figure 13B, consideration of pressure decline after one day will lead to same interpretation that means we have more rapid pressure decline in container. But following the pressure decline, e.g., for 5 days shows same pressure drop in both container and core holder containing saturated cores.

Table 9: Different amounts of oil and CO_2 used in container/core holder (oil)

	Gasoil(container)	Gasoil(coreholder)	Stockerau(container)	Stockerau(coreholder)
oil(gr)	132.94	48.93	114.09	42.94
CO2(cm3)	26.36	37.26	39.20	32.19

Table 9 presents the used amounts of gas and oil in the experiments.

A   B
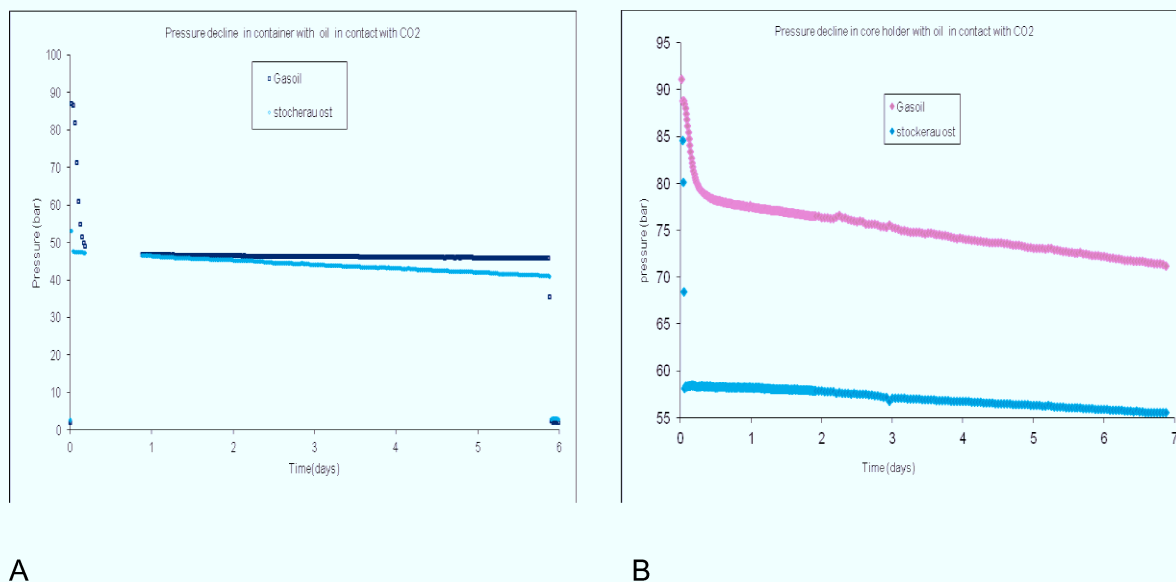
Figure 14: Oil in contact with CO2 at 40°C &100 bar in container, on the left side and in core holder, on the right side

Using core holder (Figure 14B) with higher injected CO_2 ended up to less pressure decline in both oil samples, especially in Gasoil which means lower diffusion coefficient is expected in core holders.

3.4   Experiments with Berea sandstone cores

In general, for the experiments with the core in container, three small Bereas were used, while only one Berea core is used in core holder.

To see, the difference when CO_2 diffuses only from the top (1D) and when also diffuses from the sides (2D), three same cores on each other covered with wall-tubing and left in water for a night in the distilled water and it was evacuated, to push the air molecules out of pores and be saturated with water. Three other cores on each other without wall tubing also left in water for a night such as other group (Figure 15).

After one day, the saturated cores put in the container and filled with water up to top of cores. The desired gas was injected on top of the cores and pressure decline was monitored (Figure 16).

After spending a long time on observation, we see that decreasing in the pressure continues, which can implies some mistakes during the experiment; however the pressure decline is less in the case with wall tubing as expected. (Diffusion is only vertical diffusion).
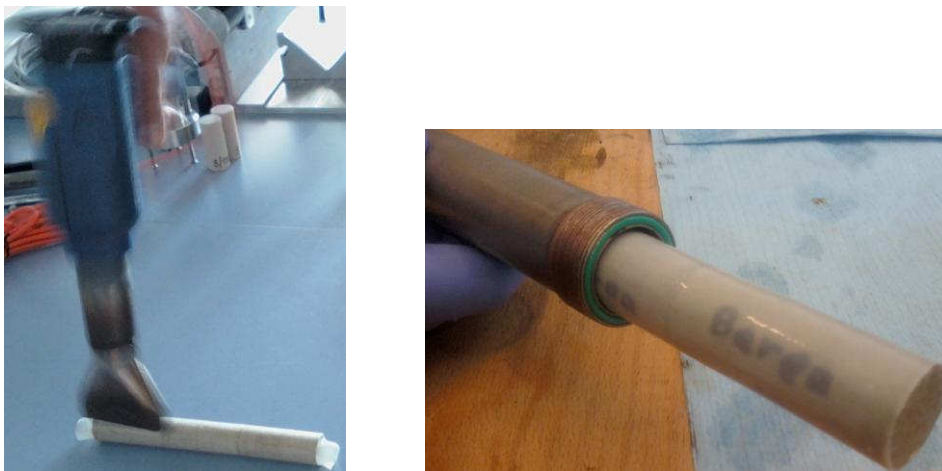
Figure 15**:** Using wall tubing around cores
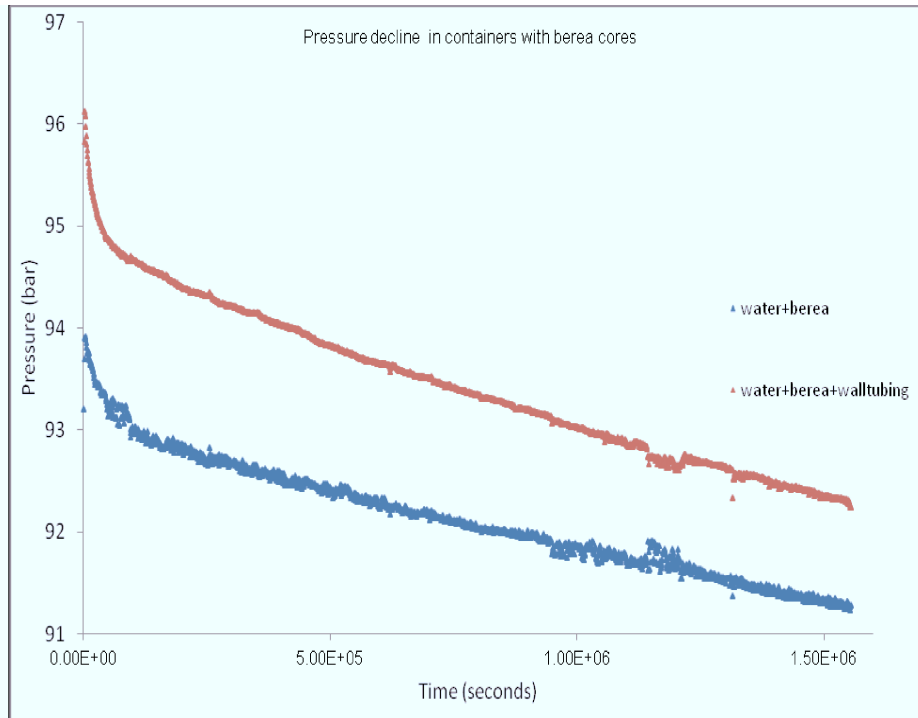
Figure 16: Berea sandstone cores in contact with CO2 at 40°C & 100 bar
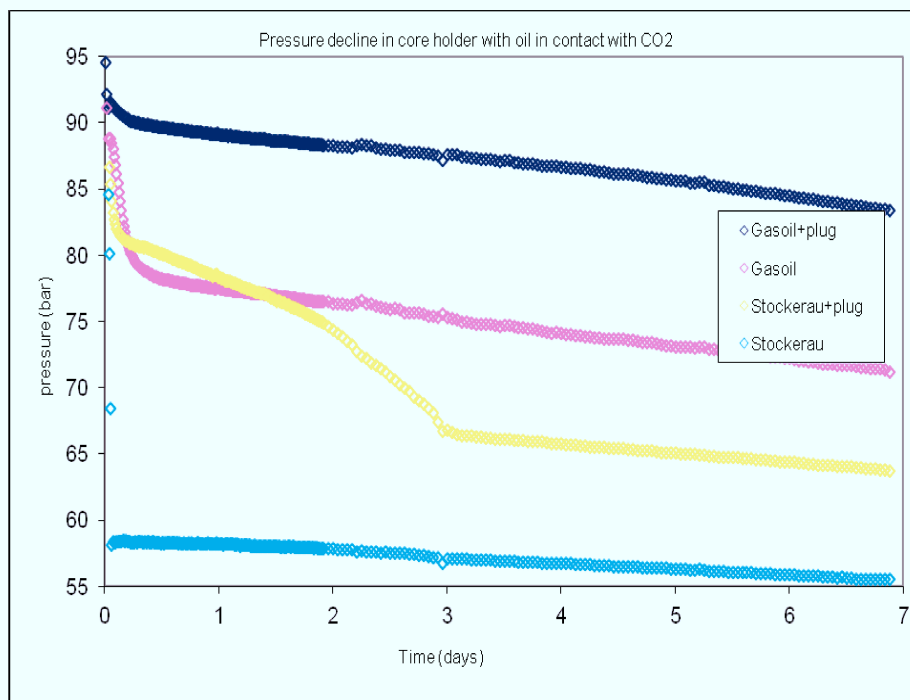
Figure 17: Oil and Berea sandstone in contact with CO2 at 40°C &100 bar

In this experiment (Figure 17), we try to compare the CO_2 dissolution in oils and oil saturated Berea cores. As we expected, in the cases with Berea core comparing with the ones without Berea cores pressure decline is slower.

35

The convex shape for saturated Berea with Stockerau, could be explained as occurring of third phase at a certain temperature and pressure.
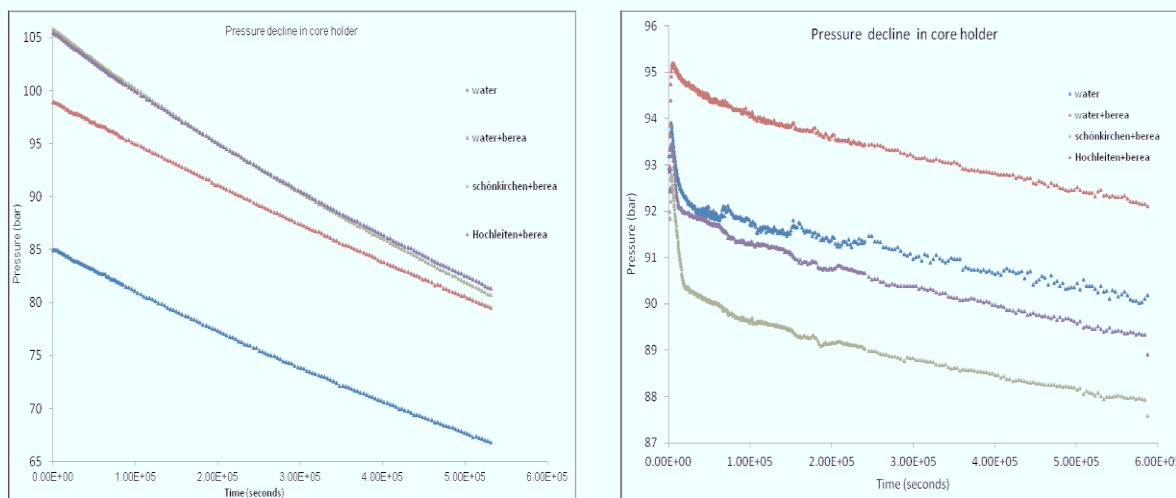
A   B

Figure 18: Water and oil saturated Berea sandstones in contact with CO2 at 80°C &100 bar, on the left side and 40°C, on the right side

The experiment in Figure 18A shows expected results. The pressure decline is slower in core holder with water saturated Bereas compare to only water filled core holders and as expected also slower in oil saturated cores rather than water saturated cores, but the large slops of the pressure declines confirms not adequate observation time.

Results of the experiments with saturated Berea cores reflect faster pressure decline for oil saturated cores rather than water saturated cores (Figure 18B) which is logical.

36

3.5   Data correlation

Unfortunately the pressure drop was not monotonously decreasing due to the temperature's difference between day and night and difference between different day's temperatures. In some situations, temperature varied up to two or three degrees (Figure 19).

Since the temperature was not exactly constant during the monitoring of the pressure, to be able to predict diffusivity coefficient properly, pressure drop had to be corrected by a model.
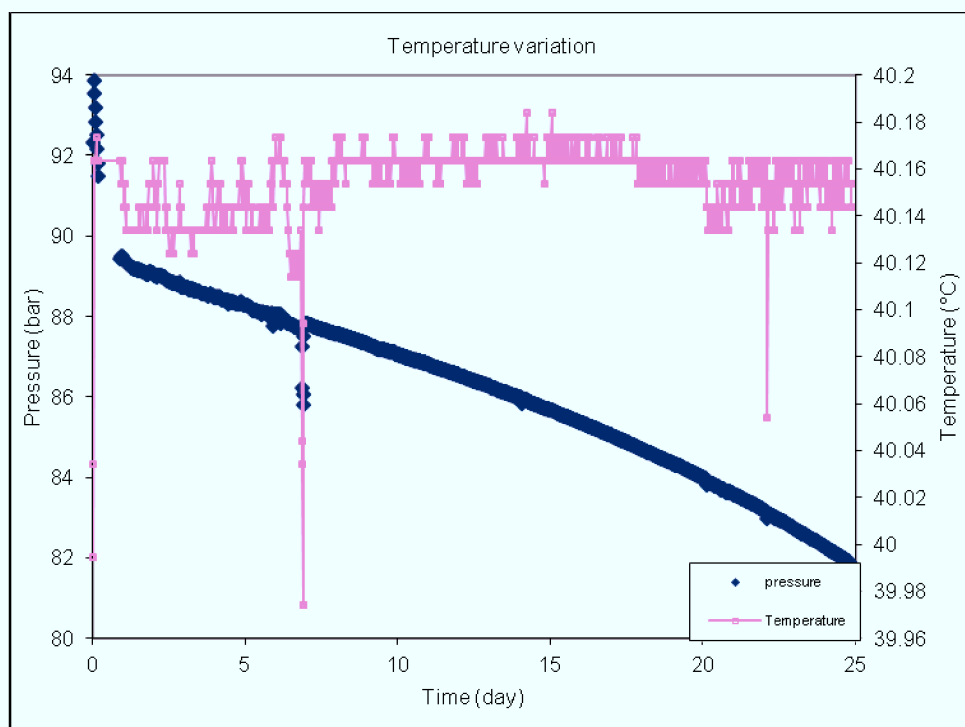
Figure 19: Temperature variation during the pressure observation at T 40°C & P100 bar for Hochleiten

3.6 Pressure models

Since temperature oscillations happened during the measuring of the pressure, and according to my mathematical model, I should work with slop of pressure decline, in this thesis I tried to define the right function for pressure decline and remove all temperature oscillations therefore, three different pressure models of linear, logarithmic and exponential has been defined to be able to get the right diffusivity as closed as given values in the literature. The Maple program was used for this purpose.

As I mentioned in previous section, natural convection speeds up the transfer of CO_2 into the water. However, it decreases with the time and after a certain time the density gradient is not large enough to sustain convection to the system and diffusion becomes the dominant mechanism for CO_2 mass transfer into the water. Therefore, for development of pressure models and calculation of the diffusivity, we focused on the late time to obtain the correct diffusion coefficient without any convection effect.

Calculating the diffusivity in the early time, would result in higher diffusivity. This would indicate a faster mass transfer rate of CO_2 into the water, due to convection at the early stages of the experiment.

3.6.1 Logarithmic pressure model

Some of the logarithmic models are presented in the next figures (Figure 20, 21). Unfortunately the results using this formulation were far away from the literature, and as the figures show sometimes they do not fit the real data as perfectly as a line function for late time pressure.

$$P = a + bt - \ln t$$

Demo Version, http://www.verydoc.com and http://www.verypdf.com
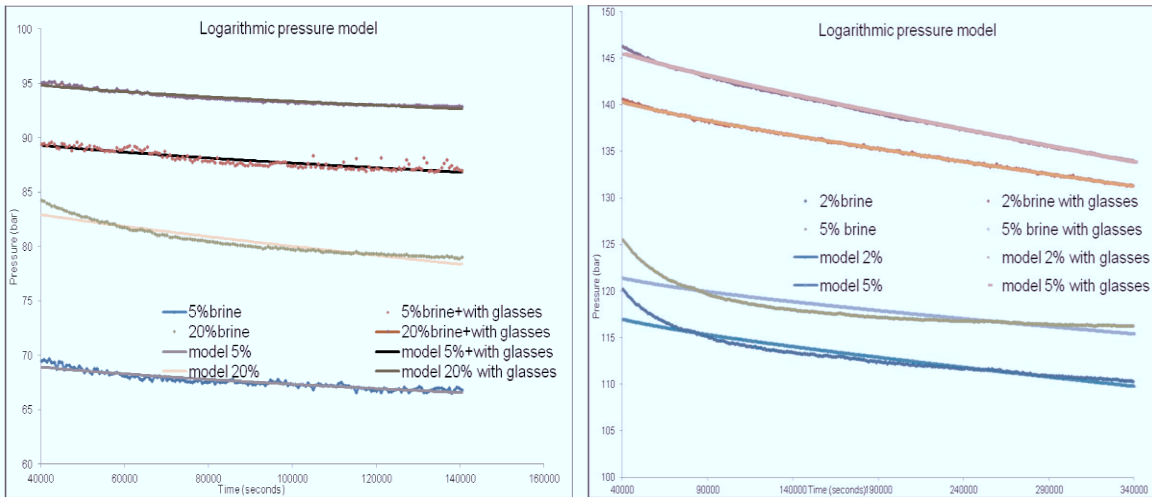
Figure 20: Logarithmic pressure model at T80°C & P100 bar, on the left side and at T40°C & P200 bar, on the right side
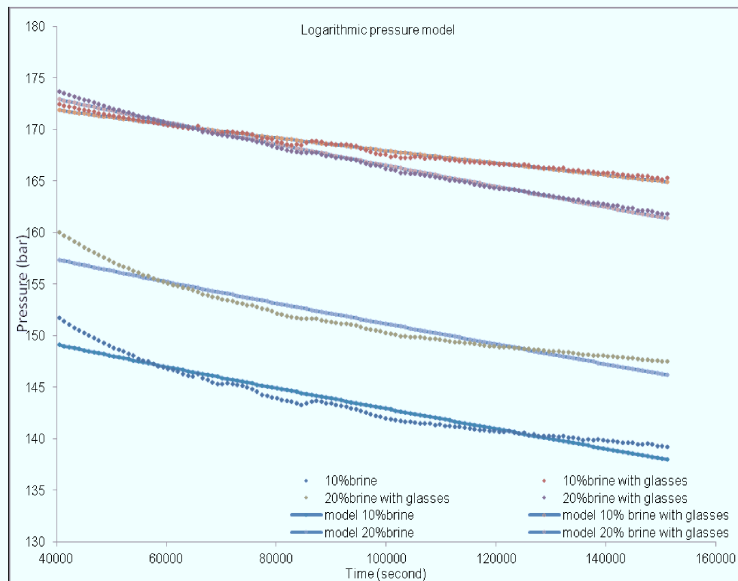
Figure 21: Logarithmic pressure model at T 40°C & P 200 bar

Unfortunately I did not have a sufficient observation time for some experiments to satisfy my models. Presented logarithmic models fit sometimes the real pressure decline very perfectly, but sometimes not really good. To compare D_{CO_2} with the values in the literature, the D_{CO_2} were calculated using logarithmic function for pressure-time relation and presented in the table 10.

Table 10: Diffusion coefficient calculated using logarithmic pressure model

water			late time(40000-60000s)	late time(40000-60000s)	
T	P	salinity	diffusivity-without glass	diffusivity-with glass	
40	50	0	4.94225E-07	7.87367E-07	m²/s
	50	1	6.01154E-07	8.41085E-07	m²/s
	50	2	4.03E-07	7.19E-07	m²/s
	50	5	4.05E-07	6.88E-07	m²/s
	50	10	2.68848E-07	5.76417E-07	m²/s
	50	20	2.01412E-07	4.03427E-07	m²/s
40	100	0	4.41295E-07	1.77083E-06	m²/s
	100	1	3.49692E-07	1.34098E-06	m²/s
	100	2	5.82104E-07	1.02748E-06	m²/s
	100	5	4.95289E-07	1.39026E-06	m²/s
	100	10	6.18821E-07	7.23625E-07	m²/s
	100	20	4.6753E-07	7.25203E-07	m²/s
	200	0	4.32E-08	4.71E-08	m²/s
	200	1	4.49E-09	1.48357E-07	m²/s
	200	2	2.28E-07	1.76E-07	m²/s
	200	5	2.55E-07	6.26E-08	m²/s
	200	10	5.05E-08	2.50322E-07	m²/s
	200	20	5.48761E-08	9.50772E-08	m²/s
60	100	0	3.08989E-07	4.47087E-07	m²/s
		5	4.0196E-07	4.85391E-07	m²/s
		10	3.84676E-07	4.18625E-07	m²/s
		20	3.99706E-07	5.09076E-07	m²/s
80	100	0	3.69E-07	4.90E-07	m²/s
		5	3.47748E-07	3.40493E-07	m²/s
		10	2.81E-07	4.79E-07	m²/s
		20	2.16569E-07	3.71614E-07	m²/s

The results are two orders of magnitude smaller than the aqueous diffusivity of CO_2. Therefore, I came up to the point to define better models in the next sections.

40

3.6.2 Exponential pressure model

Second possible pressure model was exponential. However, this model in some experiments does not fit the real pressure decline well (Figure 22), I calculated the D_{CO_2} to see the results. Some results using this model are presented in the table 11, 12 in the late time of the experiments.

$$P = a + b.\exp(ct)$$
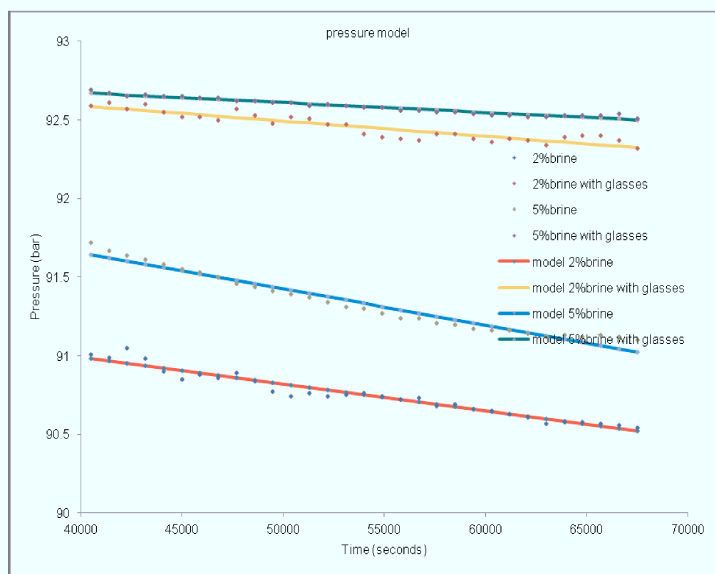
Figure 22: Exponential Pressure model at T40°C & P100

Table 11: Diffusion coefficient calculated using exponential pressure model

salinity	T	P	with glasses		Vg	water
5	40	100	2.556E-09	m2/s	30.98	79.34
5	60	100	5.83E-10	m2/s	17.2	82.01
5	80	100	1.082E-09	m2/s	27.09	78.92
10	40	100	2.065E-09	m2/s	31.78	85.43
10	60	100	7.77E-10	m2/s	16.22	82.26
10	80	100	2E-10	m2/s	7.68	82.22
20	40	100	1.7E-09	m2/s	33.67	89.5
20	60	100	6.49E-10	m2/s	17.64	86.38
20	80	100	1.27E-09	m2/s	27.09	87.84
0	40	50	6.5001E-10	m2/s	27.09	80.42
0	40	100	4.305E-09	m2/s	34.24	85.73
0	40	200	1.06E-09	m2/s	32.74	77.61
1	40	50	5.3E-10	m2/s	27.09	80.27
1	40	100	3.412E-09	m2/s	42.56	79.81
1	40	200	1.091E-09	m2/s	34.24	79.05
2	40	50	1.075E-09	m2/s	27.09	80.42
2	40	100	1.358E-09	m2/s	28.04	79.95
2	40	200	1.16E-09	m2/s	36.8	78.96
5	40	50	1.524E-09	m2/s	27.09	79.71
5	40	100	2.556E-09	m2/s	30.98	79.34
5	40	200	1.181E-09	m2/s	35.45	80.13
10	40	50	1.024E-09	m2/s	29.43	86.9
10	40	100	2.065E-09	m2/s	31.78	85.43
10	40	200	6.67E-10	m2/s	27.09	84.57
20	40	50	4.03E-10	m2/s	31.15	88.99
20	40	100	1.7E-09	m2/s	33.67	89.5
20	40	200	9.86E-10	m2/s	27.09	87.46
5	40	100	2.556E-09	m2/s	30.98	79.34
10	40	100	2.065E-09	m2/s	31.78	85.43
20	40	100	1.7E-09	m2/s	33.67	89.5
5	60	100	5.83E-10	m2/s	17.2	82.01
10	60	100	7.77E-10	m2/s	16.22	82.26
20	60	100	6.49E-10	m2/s	17.64	86.38

Table 12: Diffusion coefficient calculated using exponential pressure model

container					
T40°C&100bar					
	gasoil	schönkirchen	hochleiten	stockerau	
	1.5-5.5day	9-23 day	13-22 day	1.5-5.5day	
	3.366E-11	1.9133E-07	2.0525E-07	7.847E-07	m2/s
OIL	132.94	146.55	149.88	114.09	cm3
CO2	26.36	30.01	36.04	39.2	cm3
T80°C&100bar					
	8.1E-10	2.0408E-06	1.9274E-06	2.9989E-06	m2/s
OIL	130.45	146.25	147.03	112.75	cm3
CO2	15.64	14.09	17.87	15.85	cm3
coreholder					
T40°C&100bar					
	gasoil	stockerau			
	3.5-6.4day	2.9-6.4day			
	5.0815E-07	5.691E-07			m2/s
OIL	48.93	42.94			cm3
CO2	37.26	32.19			cm3

The calculated results also do not rise or sink logically from one experiment to another one and this pushes us to define third model.

3.6.3 Linear pressure model

Finally I decide to define linear function for the late time pressure in order to cope the temperature variation effect.

In this model, the following experiments (Table 13) are considered poor quality experiments since they did not have enough information to evaluate correct diffusivity.

Table 13: unused experiments

T	P	salinity
60	100	0,5,10,20
80	100	0,5,10,20
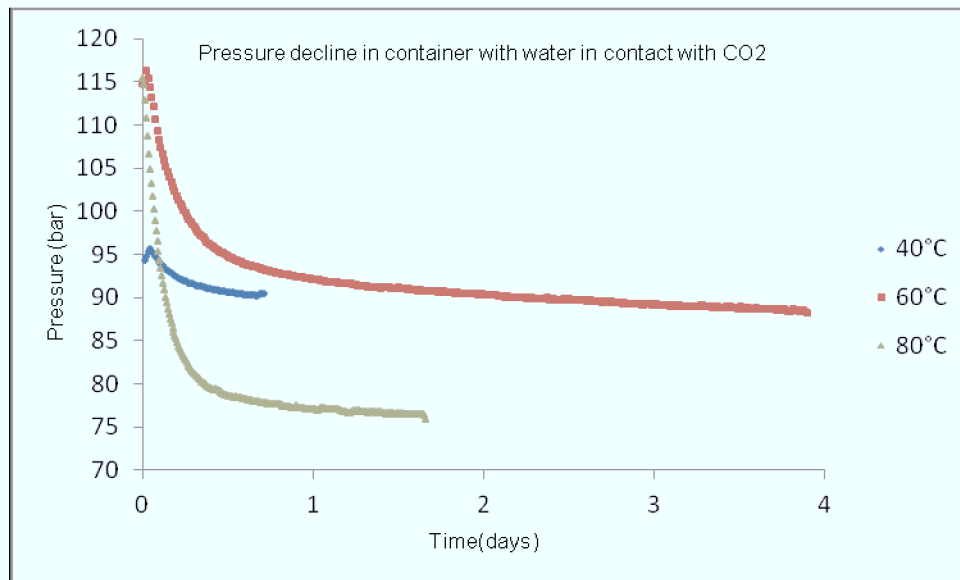
Figure 23: Pressure decline in container with water in contact with CO2 at P 100 bar

The poor quality of the experiments with 60°C and 80°C are also presented in the pressure decline related to them (Figure 23).

The linear pressure model for the late time and real data are presented on the next pages (Figure 24).

A

B

C

D

E

F

45

G

H

I

J

46
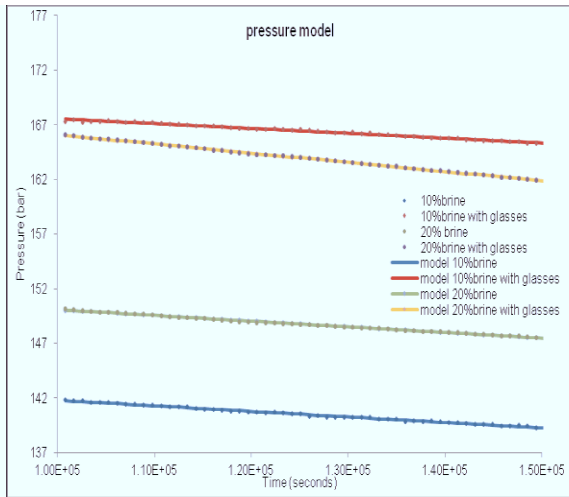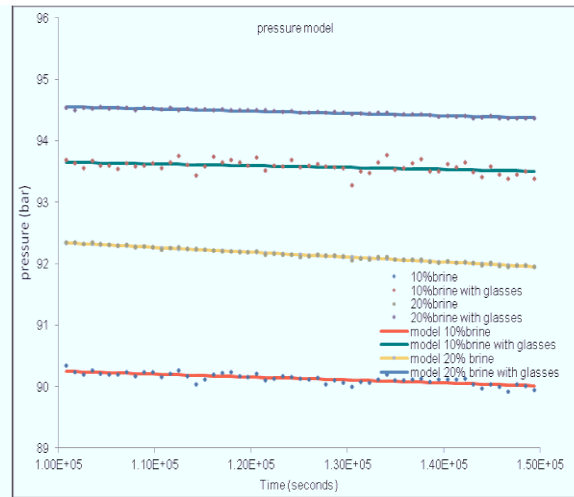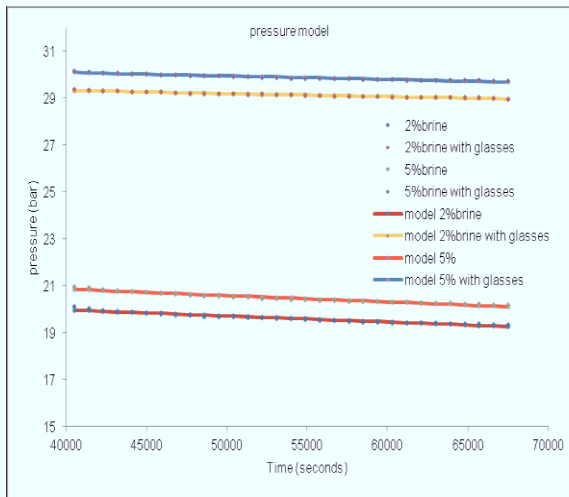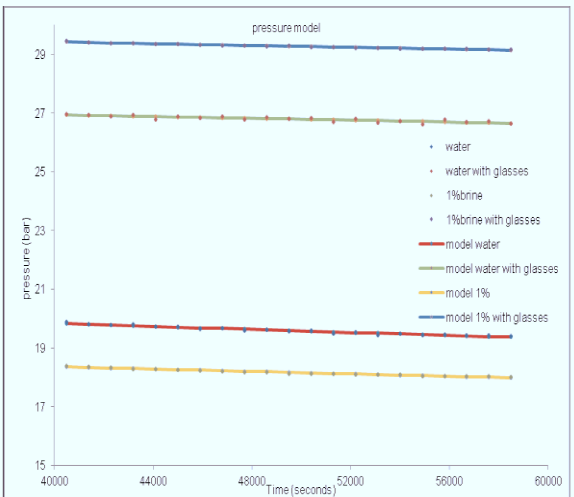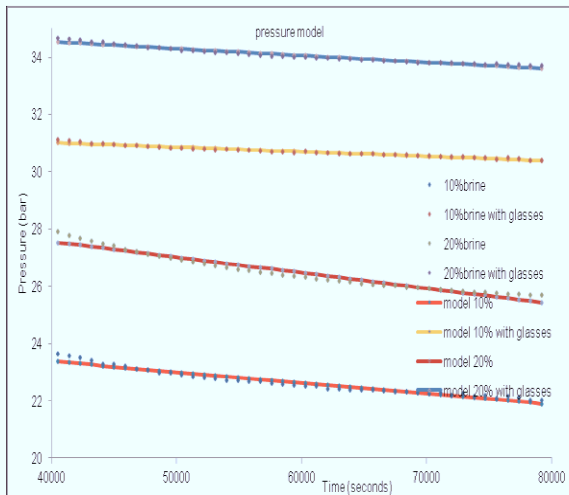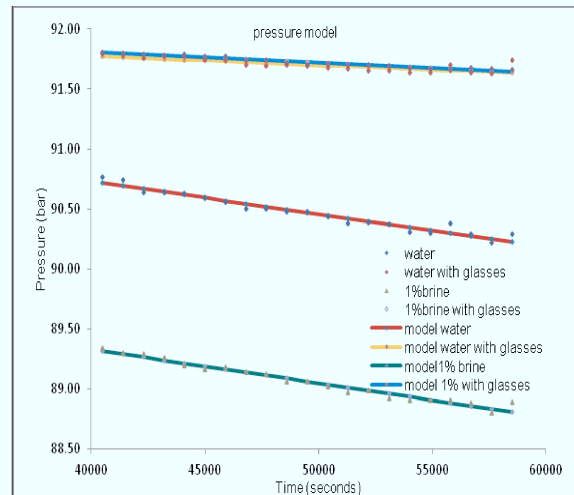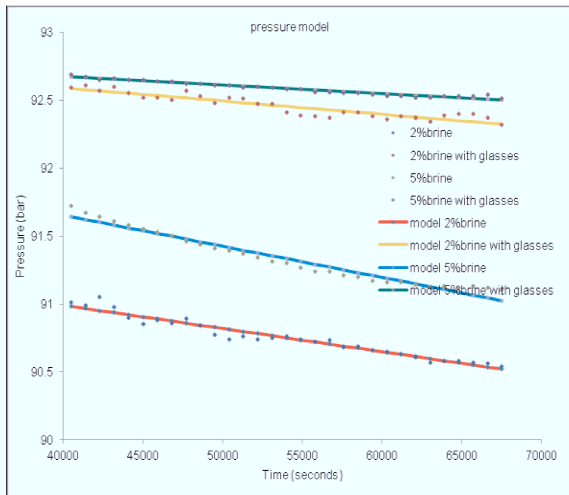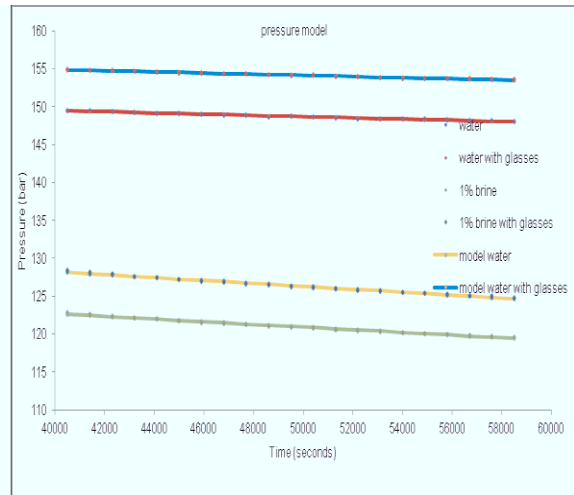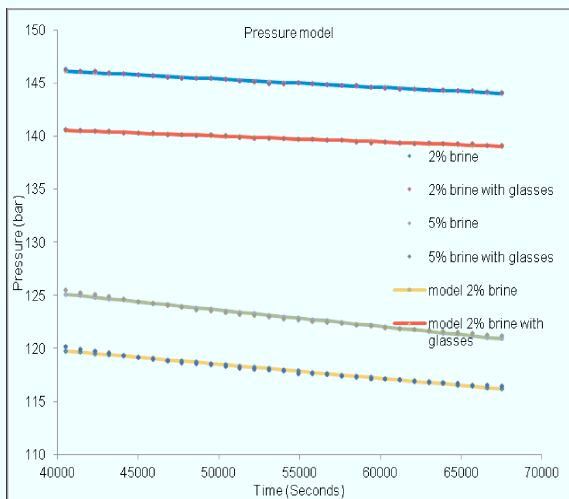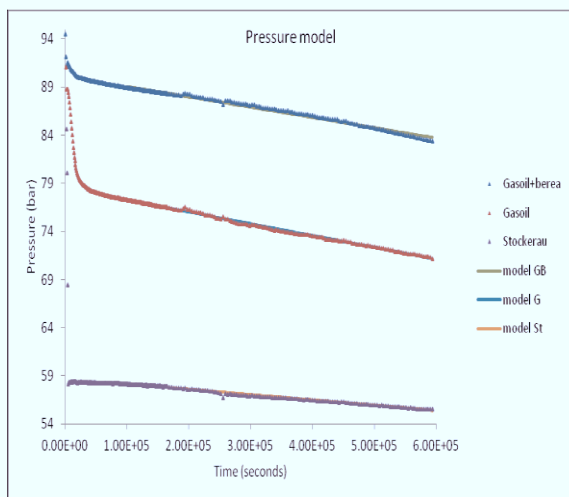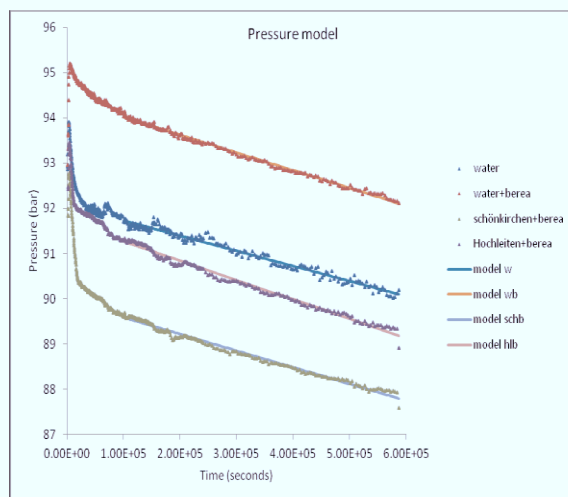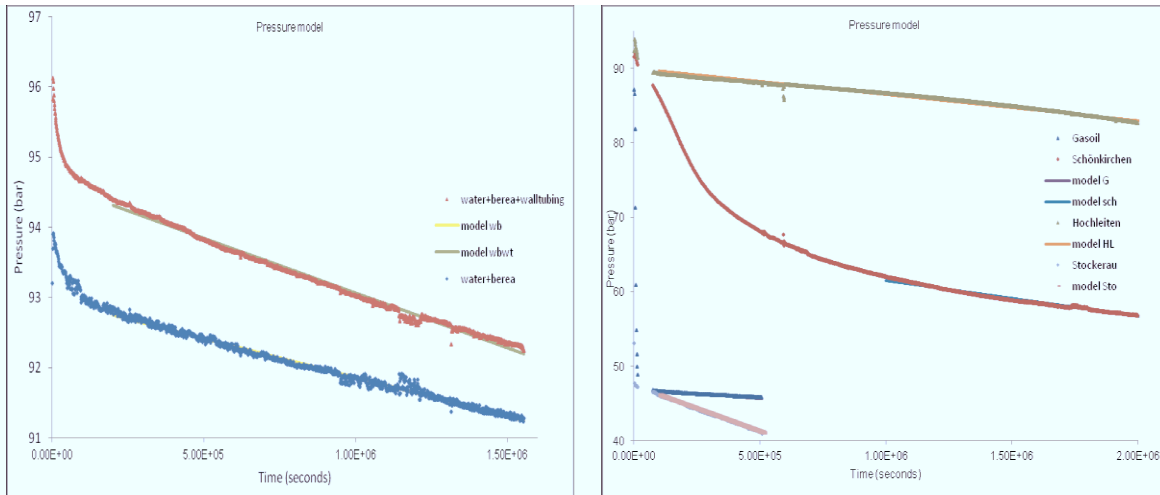
K
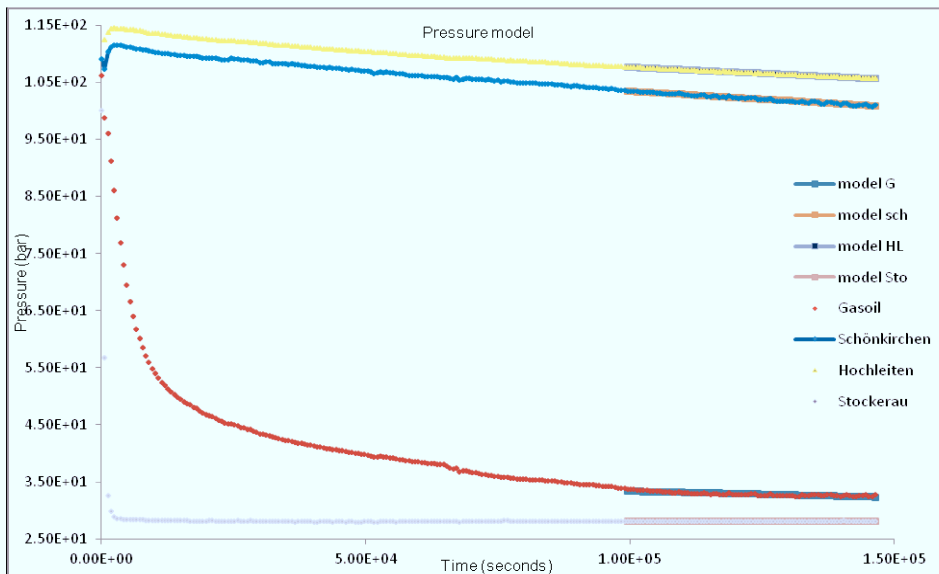
L

Figure 24: Linear pressure models

A) at T 40°C & P 200 bar for the salinity of 10 and 20 on the left side B) at T 40°C & P 100 bar for the salinity of 10 and 20 on the right side C) at T 40°C & P 50 bar for the salinity of 2 and 5 on the left side D) at T 40°C & P 50 bar for the salinity of 0 and1 on the right side E) at T 40°C & P 50 bar for the salinity of 10 and 20 left F) at T 40°C & P 100 bar for the salinity of 0 and 1 right G) at T 40°C & P 100 bar for the salinity of 2 and 5 left H) at T 40°C & P 200 bar for the salinity of 0 and 1 right I) at T 40°C & P 200 bar for the salinity of 2 and 5 left J) at T 40°C & P 100 bar in core holder K) at T40°C & P 100 bar in container L) at 80 °C and 100 bar in container

Part B of the linear pressure models, shows that the temperature variation influences largely the pressure decline of brine with 10% salinity. In part, E the influence of using glasses, plot in the left side, is observed.

47

As I mentioned before the Stockerau saturated Berea core follows different pattern than others therefore developing a linear pressure model for this type of oil was not possible. The Figure 24 shows that developing a linear model for the late time pressure fits the original plot very closely.

The diffusivity for water/brine at 40°C was also calculated using linear pressure model where the results are presented in the table 14.

Table 14: Diffusion coefficient in water/brine using linear pressure model

P(bar)	salinity	0	0	1	1	
50		8.12E-09	4.86E-09	6.52E-09	5.07E-09	m²/s
	salinity	2	2	5	5	m²/s
50		8.23E-09	4.22E-09	8.28E-09	4.75E-09	m²/s
	salinity	10	10	20	20	m²/s
50		1.2E-08	5.35E-09	1.64E-08	8.04E-09	m²/s
	salinity	0	0	1	1	m²/s
100		6.48E-08	9.60E-09	1.03E-07	1.67E-08	m²/s
	salinity	2	2	5	5	m²/s
100		9.41E-09	1.10E-08	1.18E-08	8.31E-09	m²/s
	salinity	10	10	20	20	m²/s
100		1.03E-07	5.93E-09	9.51E-09	5.13E-09	m²/s
	salinity	0	0	1	1	m²/s
200		2.4E-07	8.06E-08	2.5E-07	8.59E-08	m²/s
	salinity	2	2	5	5	m²/s
200		9.99E-08	6.04E-08	1.15E-07	8.54E-08	m²/s
	salinity	10	10	20	20	m²/s
200		5.25E-08	2.94E-08	6.55E-08	1.03E-07	m²/s

The data obtained at 60°,80°C with 100 bar had poor quality and have not been evaluated in this case. Considering the effect of using glasses in reducing convection, I will focus on these types of experiments hereinafter.
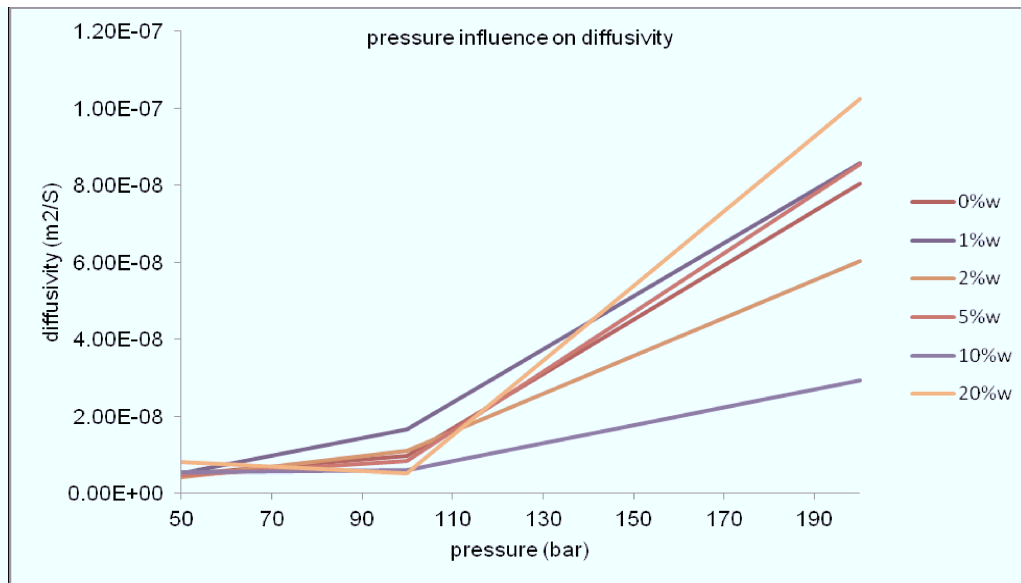
Figure 25: Pressure influence on diffusion coefficient using containers with glasses

As you see on the Figure 25, diffusion coefficient increases with the pressure the same for almost all of the salinity instead of high salinity with 20% which shows small decrease in diffusion coefficient with increasing pressure from 50 to 100 bar (ignorable) and afterward it follows also the same pattern.

The reason is, as pressure increases, the solubility of a CO_2 in water increases and viscosity of CO_2-saturated water decreases. The viscosity reduction results in the increase of the diffusivity of the CO_2 in water, in the other word the mass transfer of CO_2 increases with pressure.

Due to using of more CO_2 in core holder rather than containers, there are some differences in the calculated diffusion coefficients. Therefore, the experiments were divided into two groups; the experiments with liquid amount of much higher than CO_2 called liquid-rich and the experiments with CO_2 amount almost the same as liquid called CO_2-rich experiments (Wambui et al., 2010).

Table 15: Liquid rich experiments in container at 100 bar

T °C	experiements in container at 100 bar			
	Gasoil	Hochleiten	Stockerau ost	
40	1.2709E-09	3.25191E-09	5.84949E-09	m2/s
80	4.34173E-09	7.55271E-09	1.15092E-07	m2/s

Demo Version, http://www.verydoc.com and http://www.verypdf.com
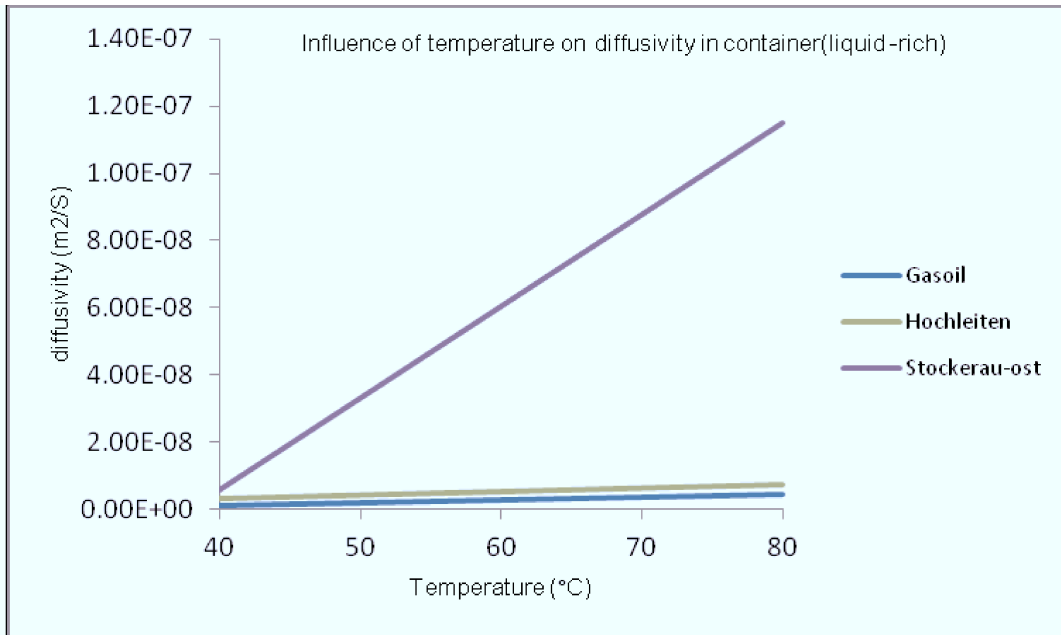
Figure 26: Influence of temperature on Dco2 in container for Liquid rich experiements

The diffusion coefficient varies directly with temperature that agrees well the presented Stokes-Einstein equation in the methodology section.

In liquid reach experiments (Figure 26, Table 15), increasing temperature results in increasing diffusion coefficient since viscosity of liquid decreases at higher temperature and makes the dissolution easier, besides at high temperatures extension of liquid molecules is lower and as temperature increases gas becomes denser while liquid becomes less dense.

Table 16:CO_2 rich experiments in core holder at 100 bar

experiments in coreholder at 100 bar					
T °C	Gasoil+core	Gasoil	Stockerau		
40	1.14E-09	1.512E-09	3.3495E-10		m2/s
	water	water+core	Schönkirchen+core	Hochleiten+core	
40	1.19E-09	1.06E-09	2.09E-09	8.70E-10	m2/s
80	6.90608E-10	7.259E-10	8.03332E-10	8.90486E-10	m2/s

Demo Version, http://www.verydoc.com and http://www.verypdf.com
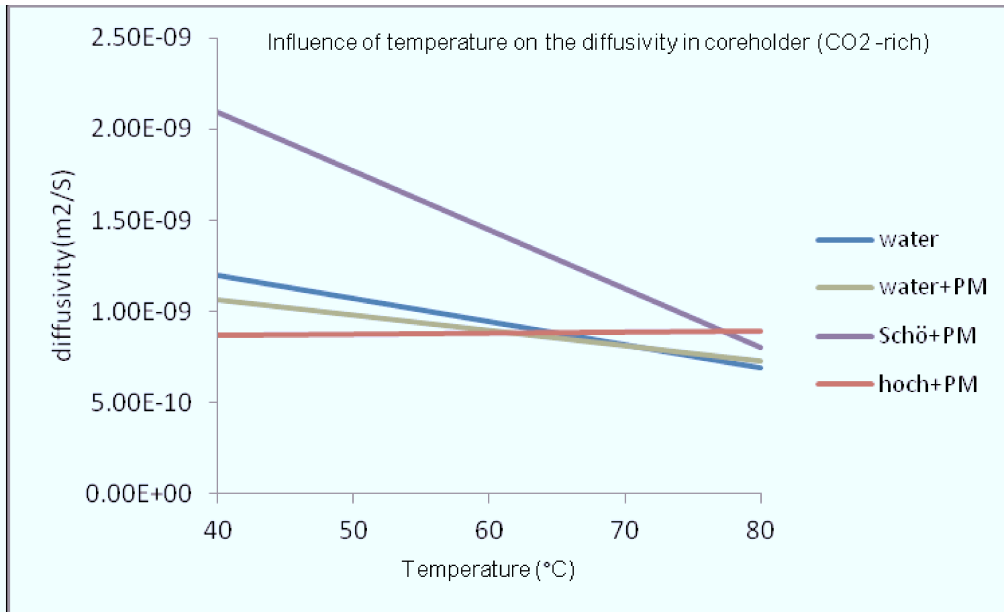
Figure 27: Influence of temperature on Dco2 in core holder for CO2 rich experiments

In CO_2 reach cases (Figure 27 and Table 16), diffusion coefficient decreases with temperature, the interpretation would be, due to large amount of CO_2 in the core holders, as the temperature increases, water starts to vapour and goes up to the CO_2 part and prevent possible pressure decline by CO_2 dissolution in water. In other words, there is mass transfer of liquid phase into gas phase

In the table 17 diffusivity of the CO_2 in oil and oil saturated core are compared.

Table 17: Diffusion coefficient in saturated cores

P bar	T °C	Schönkirchen	Sch+core	Hochleiten	HL+core	
100	40	7.87367E-07	2.09E-09	3.25E-09	8.70E-10	m2/s
100	80	1.58875E-08	8.03E-10	7.55E-09	8.9E-10	m2/s

D_{co_2} in saturated bereas are less than its diffusion coefficient in oil because of the tortuousity paths in the porous media which makes diffusion of CO_2 in saturated cores more difficult.

51

3.7   Density influence on diffusion coefficient

When we inject the CO_2 into the formation, parallel to the other influenced factors, diffusion coefficient depends on the density of the crude oil. To see the strength of this influence (Table 18 includes necessary information), D_{CO_2} is plotted over the oil density in Figure 29.

Table 18: Density influence on diffusion coefficient

	density	unit	40	80	unit
Stockerau ost	0.7230	g/cm³	5.85E-09	1.15E-07	m2/s
Gasoil	0.8382	g/cm³	1.27E-09	4.34E-09	m2/s
Hochleiten	0.9333	g/cm³	3.25E-09	7.55E-09	m2/s
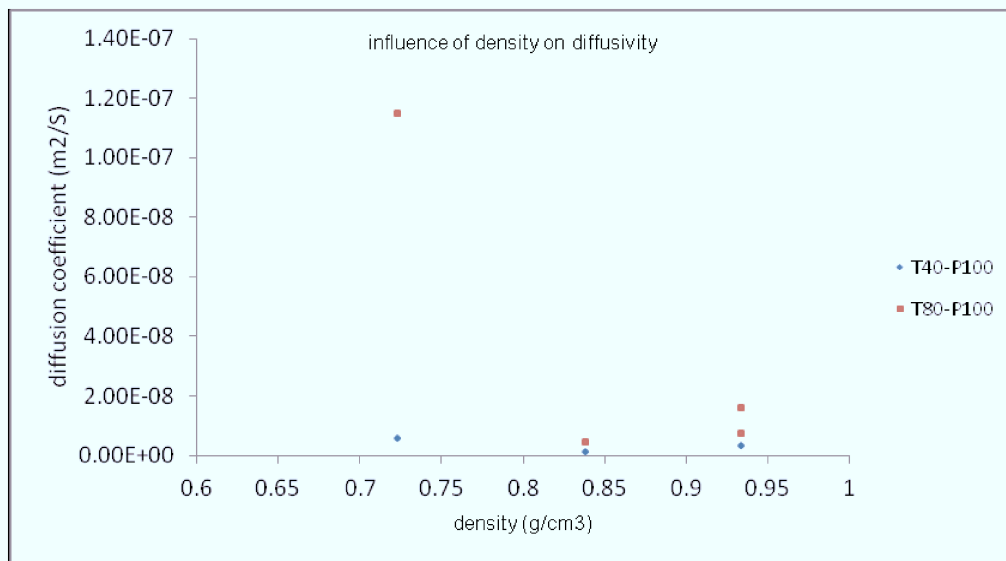
Figure 28: Influence of density on diffusion coefficient

Figure 28 shows that D_{CO_2} decreases with the density, which is logical and higher viscosity ends up in lower mass transfer.

4. Discussion

Comparison of Cussler's value (Cussler, 1976; Reid et al.,1977) for D_{CO_2} in water at 25°C, 1.92E-9 m^2/s with my value, 4.86E-9 m^2/s at Temperature of 40°C agrees well with stokes Einstein equation. Also, the results for pressure of 50, 100, 200 bar respectively with values of 4.86E-9, 9.6E-9, 8.06E-8 m^2/s show that the diffusion coefficient is increasing with pressure. D_{CO_2} in Schoenkirchen oil, 1.5E-8 m^2/s is larger than 8.03E-10 m^2/s, D_{CO_2} in Berea sandstone saturated with the same oil at the same condition of the experiment.

Developing a mathematical model and experimental set up in high pressure and temperature is a very critical and tricky job. That is the reason for a few available data in the literature at such conditions.

Pressure observation time should be increased with the salinity of the formation water and oil density.

Using thin glasses in experiments with water was useful to keep the diffusion as the only mechanism of the mass transfer in the late time behavior.

My suggestion for future works would be:

1. A horizontal set up to compare the results with experiments in vertical form.

And using

2. Less CO2/Liquid
3. Thinner containers
4. Modern and up to date equipment to keep the temperature exactly constant.

53

5. Conclusion

In this thesis, a certain amount of CO_2 gas was brought in contact with water/brine/oil and water/oil saturated Berea sandstone in container/core holder at temperature of 40, 80°C and pressure of 50, 100, 200 bar. The pressure decline has been monitored as the gas was dissolving and diffusing in liquids. A mathematical model using Ficks law was developed to determine D_{CO_2} in liquid, based on outcomes of the experiments.

The presented thesis shows importance of long pressure observations to obtain more accurate results of diffusion coefficient. The observation time depends on the pressure, temperature, salinity of water/type of oil and the amount of the injected CO_2 while the last one enhances the mass transfer of the CO_2 into liquid at early stage of the experiments. Rapid pressure decline in early stages of the experiments with larger injected gas implies that or in other words, D_{CO_2} increases with pressure proving the fact that D_{CO_2} is a strong function of the initial pressure, i.e., the initial concentration of CO_2 in the system. Using linear function was the best model for the pressure decline at late time which fits the real data exactly and gave more closed results to the literature.

The results identify also a linear relation between diffusion coefficient and temperature that agrees with Stokes Einstein equation.

Presented work obtained value of 4.86E-9 m^2/s for D_{CO_2} in water, 1.5E-8 m^2/s in Schoenkirchen oil type of Vienna basin and 8.03E-10 m^2/s in oil saturated Berea sandstone.

List of References

Cussler, E. L. (2003). *Mass transfer in fluid systems. London:* Cambridge Univ. Press.

Zhang, Y.P., Hyndman, C.L. and Maini, B.B. (1999). *Measurement of gas diffusivity in heavy oils. In Proceedings of Annual Technical Meeting , Calgary, Alberta The Journal of Petroleum Scienece and Engineering 25; 37-47. Elsevier.*

Unatrakarn, D., Asghari, K. and Condor, J. (2011). *Experimental Studies of CO2 and CH4 Diffusion Coefficient in Bulk Oil and Porous Media. In Proceedings of 10th International Conference on Greenhouse Gas Control Technologies, Saskatchewan, Canada. The Journal of Energy Procedia, 4: 2170–2177. Elsevier.*

Duan, Z. and Sun, R. (2003). *An improved model calculating CO2 solubility in pure water and aqueous NaCL solutions from 273 to 533 K and from 0 to 2000 bar. The Journal of Chemical Geology 193: 257-271. Elsevier.*

Duan, Z., Sun, R., Zhu, C., Chou, I.M. (2006). *An improved model for the calculation of CO2 solubility in aqueous solutions containing Na^+, K^+, Ca^{2+}, Mg^{2+}, Cl^-, and $SO4^{2-}$. The Journal of Marine Chemistry 98: 131-139. Elsevier.*

Duan, Z., Moller, N., Weare, J.H. (1992). *An equation of state for the CH4–CO2–H2O system: I. Pure systems from 0 to 1000 °C and 0 to 8000 bar.*

Farajzadeh, R., Barati, A., Delil, H. A., Bruining, J., and Zitha, P. L. J. (2007). *Mass Transfer of CO2 Into Water and Surfactant Solutions. The Journal of Petroleum Science and Technology, 25: 12, 1493 — 1511.*

Farajzadeh, R., Salimi, H., Zitha, P.L.J., and Bruning, J. (2007). *Numerical Simulation of Density-Driven Natural Convection in Porous Media with Application for CO2 Injection Projects. In Proceedings of EUROPEC/EAGE Conference and Exhibition, London, U.K. Society of Petroleum Engineers.*

Farajzadeh, R., Delil, H. A., Zitha, P.L.J., and Bruining, J. (2007). *Enhanced Mass Transfer of CO2 Into Water and Oil by Natural Convection. In Proceedings of EUROPEC/EAGE Conference and Exhibition, London, U.K. Society of Petroleum Engineers.*

Wambui Mutoru, J., Leahy-Dios, A., and Firoozabadi, A. (2010). *Modeling Infinite Dilution and Fickian Diffusion Coefficients of Carbon Dioxide in Water. The Journal of American Institute of Chemical Engineers AIChE J, 57: 1617–1627.*

Grogan, A.T., Pinczewski, V.W., Ruskauff, Gregory J. and Orr Jr., F.M. (1988). *Diffusion of CO2 at Reservoir Conditions: Models and Measurements. The Journal of Society of Petroleum Engineers, 3: 93-102.*

Song, L., Kantzas, A. and Bryan, J. (2010). *Experimental Measurement of Diffusion coefficient of CO_2 in Heavy Oil Using X-Ray Computed-Assisted Tomography Under*

Reservoir Conditions. In Proceedings of SPE International Conference on CO2 Capture, Storage, and Utilization, New Orleans, Louisiana, USA. Society of Petroleum Engineers.

Xia, J. (2007). Experimental determination of solubility's of CO2 in crude oil and water. (Master's thesis). Department Mineral Resources and Petroleum Engineering Chair of Reservoir Engineering, Montanuniversität Leoben.

Wang, L.-S., Lang, Z.-X. and Guo, T.-M. (1996). Measurement and Correlation of the diffusion coefficients of carbon dioxide in liquid hydrocarbons under elevated pressures. The Journal of Fluid Phase Equilibria 117: 364-372. Elsevier.

Luo, H. and Kantzas, A. (2008). Investigation of Diffusion Coefficients of Heavy Oil and Hydrocarbon Solvent Systems in Porous Media. In Proceedings of SPE/DOE Symposium on Improved Oil Recovery, Tulsa, Oklahoma, USA. Society of Petroleum Engineers .

Perry, R.H. and Green, D.W. (2007). Perry's Chemical Engineers' Handbook. McGraw-Hill

Darvish, G.R., Lindeberg, E., Holt, T., Utne, S.A. and Kleppe, J. (2006).Reservoir-Conditions Laboratory Experiments of CO2 Injection into Fractured Cores. SPE Europec/EAG Conference & Exhibition, Vienna, Austria. Society of Petroleum Engineers .

Bahar, M., Liu, K. (2008). Measurement of the Diffusion coefficient of CO_2 in Formation Water Under Reservoir Conditions: Implications for CO_2 storage. Society of Petroleum Engineers .

Renner, T.A. (1988). Measurement and Correlation of Diffusion Coefficients for CO2 and Rich-Gas Applications. Society of Petroleum Engineers .

Fenglan, Z., Shijun, H. and Jirui, H. (2011). Determination of Diffusion Coefficient and Percolation Model During CO2 Flooding, Beijing, China University of Petroleum

Yang, C. and Gu, Y. (2006). Diffusion coefficients and oil swelling factors of carbon dioxide, methane, ethane, propane, and their mixtures in heavy oil. The Journal of Fluid Phase Equilibria, 243: 64-73. Elsevier.